FOA

SMHI

Nö 95, 2000

Meteorologi

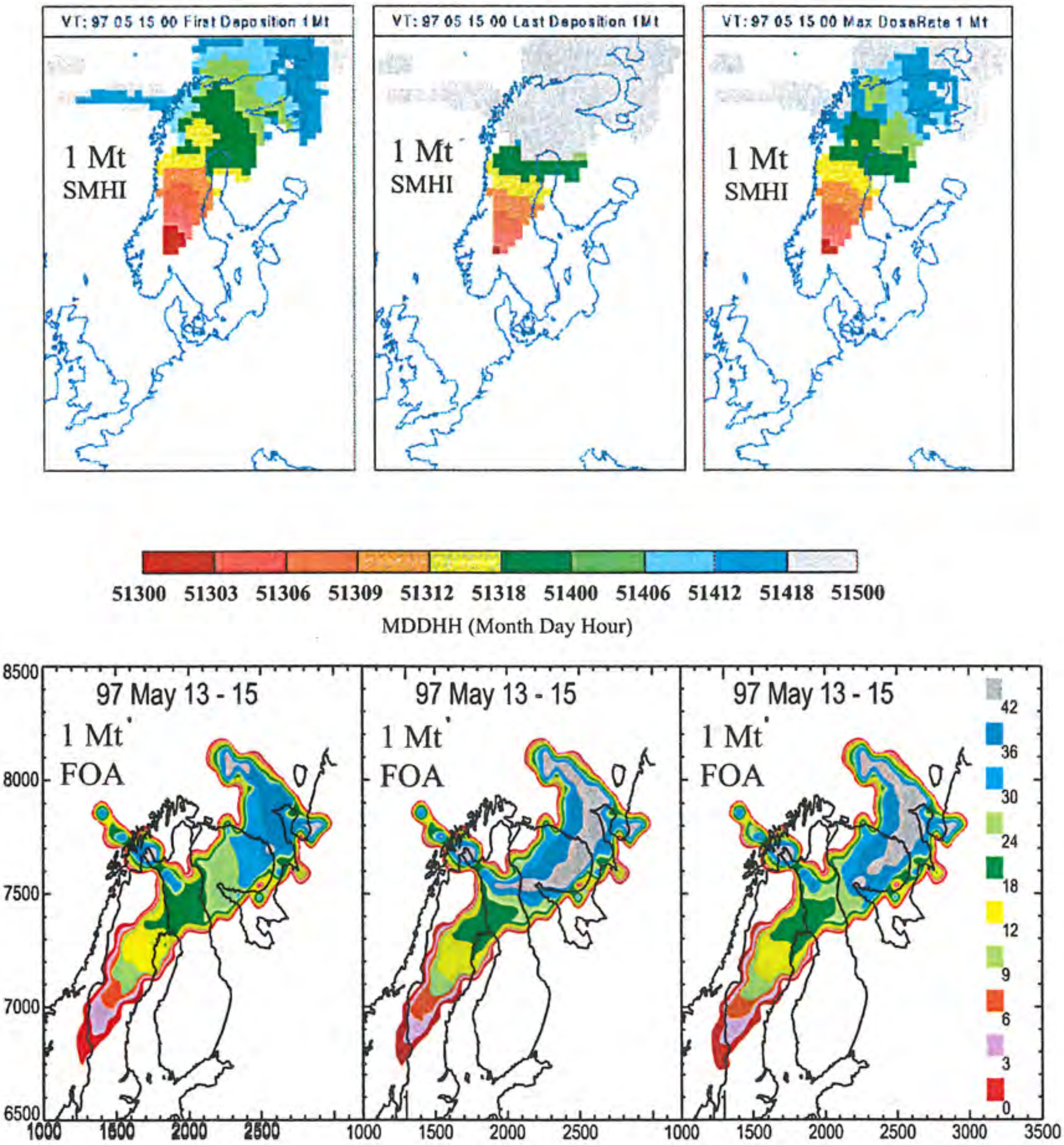

Model for Simulation of Air and Ground Contamination Associated with Nuclear Weapons

An Emergency Preparedness Model

Christer Persson and Lennart Robertson, SMHI
Lennart Thaning, FOA

With financial support from The Swedish Agency for Civil Emergency Planning, ÖCB

Meteorologi
No 95, 2000

Model for Simulation of Air and Ground Contamination Associated with Nuclear Weapons

An Emergency Preparedness Model

Christer Persson and Lennart Robertson, SMHI
Lennart Thaning, FOA

TABLE OF CONTENTS

Sammanfattning

En kärnvapenexplosion ovan mark kan medföra förödande skador på upp till någon mils avstånd från detonationspunkten p.g.a. direkta verkansformer som stötvåg, värmestrålning och initialstrålning. Men allvarliga strålskyddsproblem kan även uppträda på mycket stora avstånd genom att radioaktiva partiklar transporteras med vindarna och deponeras på avlägsna platser. Vilka områden som drabbas bestäms helt av rådande väderförhållandena och explosionstyp. Bra prognoser för när och var den radioaktiva beläggningen uppkommer är av stort värde för strålskyddsarbetet vid en verklig händelse. Sårbarhetsstudier, spel och övningar inom den civila beredskapen kräver också realistiska simuleringar. Transport och spridning i atmosfären över stora avstånd (ca 200 - 4000 km) innefattar många komplicerade processer och enda möjligheten att göra en realistisk beskrivning är att använda en datoriserad spridningsmodell.

Tillgången är mycket begränsad på mätdata som kan utnyttjas för att utveckla en spridningsmodell för simulering av kärnvapenexplosioner. Därför har i denna studie två principiellt helt olika modeller utvecklats och utnyttjats, dels PELLO vid FOA, dels MATCH vid SMHI. Modelljämförelser har givit dels förbättrad förståelse för olika processers betydelse, dels minskat risken för större fel i modellerna. PELLO-modellen är en s.k. partikelmodell (Random Displacement Model) där ett stort antal partiklar med olika storlek och egenskaper emitteras och följs. MATCH-modellen är en s.k. eulersk modell där partikelhalt och deposition beskrivs i ett högupplöst tredimensionellt rutnät.

En modul som beskriver utsläppsfördelning och partikelstorlekar för olika typer av kärnvapenexplosioner har tagits fram och utnyttjas i båda modellerna. Modellerna använder meteorologiska indata i form av numeriska analyser av uppmätta väderdata eller numeriska väderprognoser, som kan erhållas från SMHIs väderprognosmodell HIRLAM (HIgh Resolution Limited Area Model) eller den globala väderprognosmodellen vid ECMWF (European Centre for Medium Weather Forecasts).

MATCH för simulering av kärnvapenexplosioner ingår nu i SMHIs dygnet runt beredskap, där tillgång till realtids väderinformation finns. Övningar görs av berörd personal. Resultat från spridningsberäkningarna kan i realtid överföras till en skyddad hemsida på Internet, som endast berörda svenska myndigheter har tillträde till. De två spridningsmodellerna utnyttjas dessutom som simuleringsverktyg på FOA och SMHI för att ta fram underlag till olika typer av övningar och studier.

Abstract

A nuclear weapon explosion above ground can cause tremendous damage within the area of some tens of kilometres from the explosion point due to direct damage through the blast wave, thermal radiation and initial nuclear radiation. Serious radiation protection problems can also appear on very large distances, due to large amounts of radioactive particles being transported by the winds and deposited in areas far away from the explosion. Which areas to be affected are entirely determined by the character of the explosion and the present weather situation. In such situations the possibility to simulate and forecast in an accurate way the transport and deposition of radioactive substances, caused by the nuclear explosion, can be of fundamental importance in the radiation protection work. Studies of vulnerability and exercises within the civil preparedness also demand realistic simulations. Transport and dispersion in the atmosphere over large distances (ca 200 – 4000 km) includes many complex processes and the only possibility to make a realistic description is to use a computerised dispersion model.

The access to measured atmospheric chemistry or radiological data, which can be utilised for the development of a dispersion model for nuclear weapon explosions, is very limited. Therefore two in principal different models have been developed and utilised in the present study, on one hand PELLO at FOA, on the other hand MATCH at SMHI. The model comparisons have given both better understanding of the importance of different processes and reduced the risk for severe errors in the models. The PELLO model is a so-called particle model (Random Displacement Model) in which a large amount of particles, with different sizes and characteristics, are emitted and traced. The MATCH model is basically a so-called Eulerian model, where concentration of particles and deposition are described in a high-resolution three-dimensional grid.

A module describing the emission distribution of particle sizes at different types of nuclear weapon explosions has been formulated and is used in both models. The meteorological input data to both models is numerical weather analyses and forecasts. This weather information can be obtained from the European scale HIRLAM (HIgh Resolution Limited Area Model) weather forecast model at SMHI or from the global model at ECMWF (European Centre for Medium Weather Forecasts).

The MATCH model, adjusted to simulations of explosions of nuclear weapons, is now included in the 24h preparedness at SMHI where real time weather data is available. Exercises are performed for the involved staff. Results from dispersion calculations can in real time be transmitted to a homepage on Internet with restricted access only for involved Swedish authorities. Besides, both dispersion models can be utilised as simulation tools at FOA and SMHI to produce the basis for different types of exercises and studies.

1 Introduction

A nuclear weapon explosion above ground can cause tremendous damage within the area of some tens of kilometres from the explosion point due to direct damage through the blast wave, thermal radiation and initial nuclear radiation. Serious radiation protection problems can also appear on very large distances, due to large amounts of radioactive particles being transported by the winds and deposited in areas far away from the explosion. Which areas to be affected are entirely determined by the character of the explosion and the present weather situation. In such situations the possibility to accurately simulate and forecast the transport and deposition of radioactive substances, caused by the nuclear explosion, can be of fundamental importance for the radiation protection work.

Studies of vulnerability and exercises within the civil preparedness also demand realistic simulations. Transport and dispersion in the atmosphere over large distances (ca 200 – 4000 km) includes many complex processes and the only possibility of making a realistic description is to use a computerised dispersion model.

2 Purpose

The purpose of the present study is to develop a model system able to simulate and forecast of the atmospheric transport and dispersion of radioactive substances caused by nuclear weapon explosions. It shall be possible to use the model system in real time for emergency preparedness as well as for studies of vulnerability and for exercises within the civil preparedness which demand realistic simulations.

3 Meteorological data

The access to meteorological information of high quality from Numerical Weather Prediction (NWP) models is of fundamental importance for the applications of real time atmospheric transport models. In this study the transport models have been designed to use analyses or forecasts from the ECMWF (European Centre for Medium Weather Forecasts) or the HIRLAM (HIgh Resolution Limited Area Model) weather prediction models. The weather prediction model HIRLAM is developed in a joint project between the Nordic countries, Ireland, Netherlands and Spain. Today also the three Baltic countries, Estonia, Latvia and Lithuania, are included in the HIRLAM co-operation.

In the emergency preparedness system, described below, the necessary meteorological analyses and forecasts are, for the time being, obtained only from the Swedish operational applications of the numerical weather prediction model HIRLAM. There is a possibility, in the future, to include also ECMWF meteorological data in the real-time preparedness at SMHI. In certain situations this can be of great importance since the ECMWF data covers a larger area (the whole earth) and has a larger extension in time (240 hours compared to 48 hours for a HIRLAM forecast). However, that demands an increase in data transfer capacity between ECMWF and SMHI compared to present state.

4 Emission scenarios for nuclear weapons

The nuclear weapon emission scenarios given in Table 4.1 and Table 4.2 are applied for model calculations within the present study and as default values for the emergency preparedness.

Table 4.1. The following values for the initial size of the radioactive cloud, after plume-rise and stabilisation, have been used. The cloud is assumed to have the form of a cylinder.

Explosive yield (kiloton)	Thickness of cloud (km)	Radius of cloud (km)	Height to centre of cloud (km)
1	1.0	0.6	1.5
10	2.5	1.4	3.5
100	6.1	3.2	9.0
1000	10.0	8.5	15.0

Table 4.2. Assumed initial activity in the cloud.

Explosive yield (kiloton; kt)	Activity (Bq)
1	2×10^{19}
10	2×10^{20}
100	2×10^{21}
1000 [1]	1×10^{22}

The assumed activity distribution is a function of particle radius following the AFIT model (Bridgeman and Bigelow, 1983) which, in spite of its relative simplicity, is able to reproduce the results of the much more complicated DELFIC model (Norment, 1979). The comparison is made for low yield surface[2] bursts over deserts. According to the AFIT model the activity distribution is the sum of two log-normalised distributions. One describing the distribution of activity within the particles, proportional to volume (vol), and another describing the activity associated with the surface (area) of the particles. The frequency function for the activity then yields:

$$A(r) = A_t\left[f \cdot F_{vol} + (1.-f)F_{area}\right]$$

where

$$F_{vol}(r) = \frac{1}{\sqrt{2\pi} \cdot \ln(s) \cdot r} e^{-0.5\left(\frac{\ln(r)-\ln(r_3)}{\ln(s)}\right)^2}$$

and

[1] The reason why activity from a 1000 kt explosion is less than 10 times activity from a 100 kt explosion is that the radioactive material is mainly generated by fission. For very large explosive yields, such as 1000 kt, at least 50% of the energy come from fusion.

[2] A surface burst happens when the fireball, generated by the explosion, abuts or touches the surface of the earth. Material from the earth is then vaporised and later, at higher altitudes condensed into particles, which can carry the radioactivity. A surface burst is the type of explosion which cause the most severe effects when it comes to transport and deposition of radioactive particles

$$F_{area}(r) = \frac{1}{\sqrt{2\pi} \cdot \ln(s) \cdot r} e^{-0.5\left(\frac{\ln(r)-\ln(r_2)}{\ln(s)}\right)^2},$$

A_t is the total activity

and
$\mathbf{r_2} = 7.33$ µm; $\mathbf{r_3} = 50.1$ µm; $\mathbf{s} = 4$; $\mathbf{f} = 0.66$.

Thus, we are using two log-normalised particle distributions, as indicated above, with the same amount of activity in each particle, but with different values for the two distributions. This is a more convenient way than creating a particle distribution, which corresponds to the real size of the particles and having the activity of the particles dependent on particle size.

The sedimentation velocity as a function of the particle radius is calculated according to Näslund and Thaning (1991) with the assumption that the particle density is 2880 kg/m^3.

5 Atmospheric transport models

Transport and dispersion in the atmosphere over large distances (ca 200 – 4000 km) includes many complex processes, such as emission, transport, diffusion and sink processes, and the only possibility to make a realistic description is to use a computerised dispersion model. The specific problem of describing the atmospheric transport and deposition of radioactive substances created in a nuclear weapon explosion involves the description of processes in a very deep layer of the atmosphere (troposphere and stratosphere up to about 25 km). In most national and international atmospheric transport model studies made so far, mainly focused on traffic and industrial air pollutants, only the lower layers of the troposphere, and especially the planetary boundary layer of approx. 1-2 km depth, are described. Some model studies for the whole of the troposphere (up to about 10 km), often using ^{222}Rn as a tracer, have also been presented, e.g. Robertson et. al. (1999). However, in literature only limited information concerning transport modelling in such deep layers as studied here is present. Either global fallout and deposition on a very long time scale (many years) using simple box models for the atmosphere (e.g. Peterson, 1970) or the effects of early fallout (time scale 3-12 hours) based on idealised fallout patterns and simplified meteorological input (e.g. Arkin et al, 1982), are studied. Moreover, measured data useful for design and calibration of transport models describing the radioactive contamination caused by nuclear weapon explosions are very sparse. Therefore, this project has been designed to include the development and application of two, in principle quite different atmospheric transport models, the PELLO model at FOA (a particle model) and the MATCH model (basically an Eulerian model) at SMHI. These two models have then been compared internally regarding descriptions of processes, different explosion scenarios and different weather situations, in order to understand the atmospheric transport problem of nuclear weapon radioactive contamination and insure that no serious mistakes are present in the model formulations.

5.1 The PELLO model - FOA

PELLO is an acronym for Particle model in an Eta, Latitude, Longitude co-ordinate system The main part of the development was carried out in a Degree project for the Master of Science in engineering Physics, at the University of Umeå, Sweden (Lindqvist, 1999, in Swedish).

5.1.1 Purpose

The model was designed to meet two requirements:

1. It should describe transport, dispersion and deposition on the regional scale, using real weather data, forecasted or analysed, from ECMWF or SMHI (HIRLAM data).
2. It should use the weather data in a way as direct and efficient as possible. A main point here was to develop a model that used the same system of vertical co-ordinates as was used at ECMWF and SMHI.

5.1.2 System of co-ordinates

In the horizontal the model use, latitude and longitude on an ellipsoid with major axis = 6377397.154 m and eccentricity = 0.00667437252, as co-ordinates. In the vertical an η-system, i.e. a reduced pressure system (σ-system) close to ground, a pressure system (p-system) at the top and a linear combination of the two in-between (details of the η-system can be found e.g. in Louis, 1986), see also Figure 5.2.

5.1.3 Modul formulation

The model is a Random Displacement Model (RDM) which is the Lagrangian analogue to the Eulerian K-model.

In the vertical the K_z –values are based on Lange (1989) where K_z is a weighted sum of a boundary layer value (K_z^{bl}) and free atmosphere value (K_z^{tropo}) according to:

$$K_z = H(z)K_z^{bl}(z) + [1 - H(z)]K_z^{tropo}$$

where $K_z^{bl}(z) = \frac{ku_* z}{\phi_z} e^{-cz/z_{PBL}}$

$$\phi_z = \left[1 + a\frac{z}{L}\right]^b; \quad a = \begin{cases} -15 & , 1/L < 0 \\ 0 & , 1/L = 0 \\ 4{,}5 & , 1/L > 0 \end{cases}; \quad b = \begin{cases} -0.25 & , 1/L < 0 \\ 1 & , 1/L \geq 0 \end{cases}; \quad c=4$$

and $H(z) = e^{-(z/c_2 z_{pbl})^8}$, $c_2 = 1.5$, $K_z^{tropo} = 1$ m^2/s; L is the Obukhov length and Z_{pbl} is the boundary layer height.

The horizontal value of the eddy viscosity follows the ideas of Draxler (1976) and Nasstrom (1995), yielding:

$$K_H = \frac{\sigma_v^2 t\left[1+\frac{d}{2}\left(\frac{t}{\tau_H}\right)^{1/2}\right]}{\left[1+d\left(\frac{t}{\tau_H}\right)^{1/2}\right]^3}$$

where d = 0.36, τ_H = 160 s, $\sigma_v = 2.5 \cdot u_* e^{-z/z_{PBL}}$ and t is the age of the particle.

This gives a reasonable increase in time for K_H within the boundary layer and in the lower part of the troposphere. However, at high altitudes the values of K_H become negligible and the horizontal diffusion is only due to the variation in space and time of the mean wind field. For a release at very high altitudes this feature may underestimate the horizontal diffusion, at least in the beginning when the cloud is on the sub-grid scale. However, some numerical tests with rather large values of K_H indicate that the effect is very small.

5.1.4 Determination of the friction velocity and the boundary layer height

The Obukhov length (L) and the friction velocity u_* are determined by finding values matching the Monin-Obukhov similarity theory with the wind speed at 10 m height (U_{10}), the roughness length (z_0) and the sensible heat flux at the ground (H_0) as input. The method is not without problems e.g. in the stable case there are generally two solutions of which the one with the largest u_* (also largest L) is chosen. In some situations with low wind speed, there is no solution – in those cases the absolute value H_0 is decreased until a solution appears.

In stable and neutral situations boundary layer height (z_{pbl}) is determined according to Zilitinkevich (1996):

$$\left(\frac{fz_{PBL}}{C_n u_*}\right)^2 + \frac{z_{PBL}}{C_s kL} + \frac{Nz_{PBL}}{C_i u_*} + \frac{z_{PBL}|f|^{1/2}}{C_{sr}(u_* kL)^{1/2}} + \frac{z_{PBL}|Nf|^{1/2}}{C_{ir} u_*} + \frac{z_{PBL}}{h_a} = 1 + C_e \frac{w_h}{u_*}$$

where w_h is the vertical velocity (m/s) at z = z_{PBL}; f is the Coriolis parameter;
k is von Karman's constant; N is the Brunt Väisälä–frequency
and C_n=0.5; C_s=10; C_i=20; C_{sr}=1.0; C_{ir}=1.7; C_e=0.3 and h_a= 15 km

The corresponding value in unstable situations is based on the same ideas as used in the SMHI model MATCH (Robertsson et al, 1996) and defined as the altitude where the Richardson value (R_i) has grown to 0.25. R_i is defined according to:

$$\mathrm{Ri} = \frac{gz}{|v_H|^2}\frac{\theta_z - \theta_s}{\theta_1}$$

where $\theta_s = \theta_1 + 8.5\frac{H_0}{\rho c_p w_m}$; $w_m = (u_*^3 + 0.6 w_*^3)^{1/3}$; $w_* = \frac{gH_0}{\rho C_p T} z_{PBL}$ and θ_1 is the potential temperature at the lowest model level.

5.1.5 Deposition

Dry deposition

The settling velocity (v_s) is determined with the assumption of spherical particles and follows Näslund and Thaning (1991).

The probability for deposition of a particle (P_{dep}), which in a time step ends up beneath the ground, is calculated according to Näslund and Karlsson (1995):

$$P_{dep} = \sqrt{2\pi} \cdot \frac{v_d}{\sigma_w}$$

Where v_d, the deposition velocity, is the sum of two parts: the settling velocity (v_s) and a part describing the surface processes of dry deposition.

$$\sigma_w = 1.7 \cdot u_*$$

A particle, which in a time step is moved to beneath the ground but should not be deposited is instead reflected.

Wet deposition

The wet deposition in the model is also based on the idea that a particle that finds itself in an environment with precipitation should be exposed for certain probability (P_{wdep}) to deposit. This probability is calculated according to:

$P_{wdep} = (1 - e^{-\Lambda \cdot \Delta t})$, where the washout coefficient Λ is a function of the particle radius and the precipitation intensity:

$r < 1.4\ \mu m$: $\Lambda = a_0 \cdot q^{0.79}$

$1.4\ \mu m \leq r < 10\ \mu m$: $\Lambda = (b_0 + b_1 r + b_2 r^2 + b_3 r3) \cdot f(q)$

$r \geq 10\ \mu m$: $\Lambda = f(q)$

where

$f(q) = a_1 q + a_2 q$ and q is the precipitation rate (mm/h)
$a_0 = 8.4 \cdot 10^{-5}$; $a_1 = 2.7 \cdot 10^{-4}$; $a_2 = -3.618 \cdot 10^{-6}$,
$b_0 = -0.1483$; $b_1 = 3.220133 \cdot 10^5$; $b_2 = -3.00626 \cdot 10^{10}$; $b_3 = 9.34458 \cdot 10^{14}$.

The precipitation rate is calculated from the input weather data. The calculation is based on the idea that when saturated air is transported upwards condensation will take place due to the adiabatic cooling. If it is assumed that all condensed water will fall out as precipitation the intensity can be written:

$$N_i(z) = \int_z^{\infty} w\left(\frac{dq_s}{dz}\right)_f \rho dz$$

where $N_i(z)$ is the intensity of the precipitation ($kg/m^2/s \equiv mm/s$) at level z; w is the vertical velocity (> 0); q_s is the saturation value of the specific humidity; ρ is the density of the air and f denotes moist-adiabatic conditions.

The method is rather crude and can only be expected to catch large scale precipitation patterns. In order to get realistic precipitation rates, the air is assumed to be saturated at 80% relative humidity.

5.1.6 Time step

The time step is chosen in such a way that the maximum displacement allowed for any particle is half of the grid length. The test is performed in all three dimensions.

5.2 The MATCH model - SMHI

MATCH is an acronym for Multi-scale Atmospheric Transport and Chemistry model which has been developed over several years at SMHI initially for acidifying air pollution studies (Persson et.al.,1994) and further developed and extended to the whole troposphere (Robertson et.al.,1999). MATCH is essentially an Eulerian model but has a hybrid Lagrangian particle sub-module for the initial phase of a point source release. Modules for handling nuclear weapon explosion scenarios are the most recent extensions of MATCH.

5.2.1 Purpose

The general MATCH model system, including several different model options, is designed to be an all purpose model system to meet the following requirements:

1. It should describe transport, dispersion and deposition on various scales using real-time weather data, forecasted or analysed, from HIRLAM or ECMWF, with options to be combined with meso-scale detailed analyses of specific boundary layer parameters.
2. It should include modules for sedimentation of particles of different sizes, simplified sulphur and nitrogen chemistry as well as more complex chemistry schemes.
3. The model should be possible to initialise with a Lagrangian particle model.

5.2.2 System of co-ordinates

The MATCH model is designed to adapt to the grid projection and resolution that the input meteorological data are defined upon. So far the following projections can be handled: polar-stereographic projection, UTM and RAK co-ordinates, and spherical co-ordinates (ordinary latitude-longitude grid or rotated spherical co-ordinates). The vertical resolution is identical to the η-co-ordinates used by HIRLAM and ECMWF. Figures 5.1 and 5.2 show the model area used for emergency response and the vertical resolution, respectively.

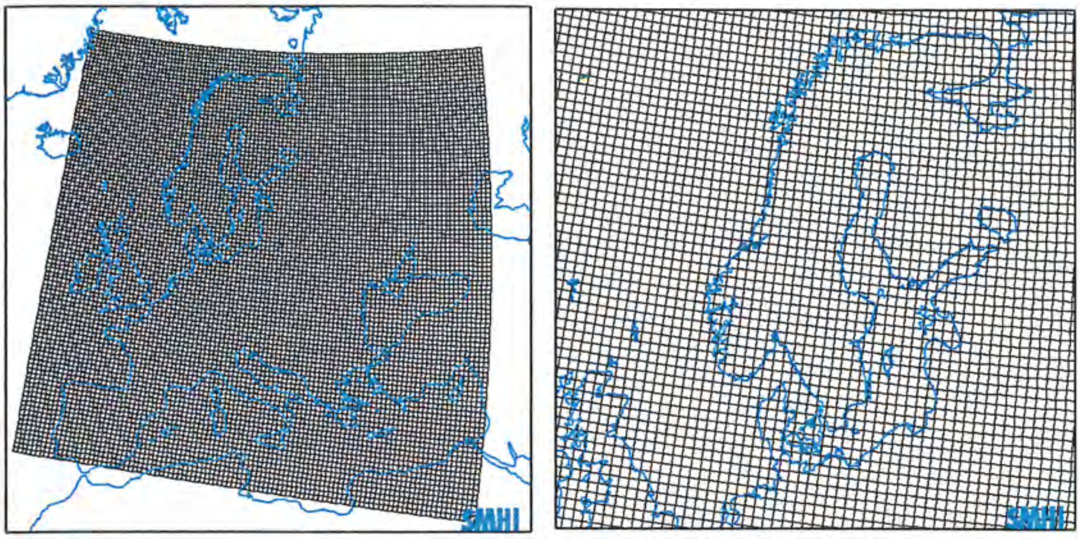

***Figur 5.1**. Model area used. The right panel is a close up to illustrate the resolution.*

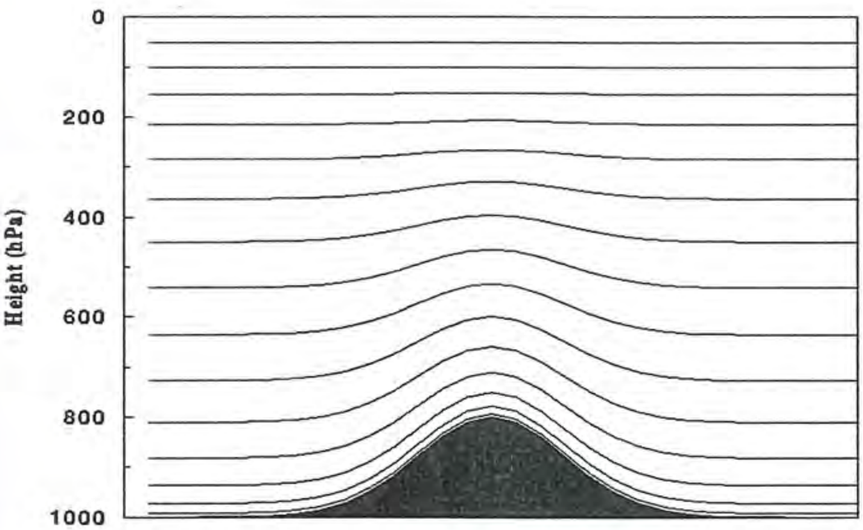

***Figur 5.2**. Vertical separation of layers in a so called η co-ordinate system.*

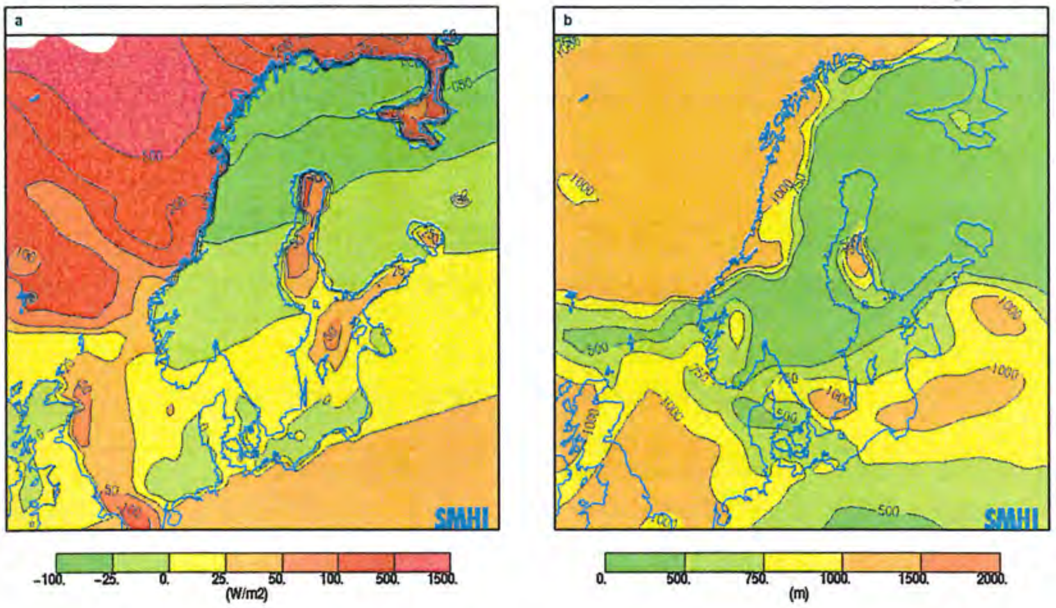

***Figur 5.3**. Example of calculated sensible heat flux (a) and boundary layer height (b).*

5.2.3 Model formulation

The MATCH model is a hybrid Lagrangian-Eulerian model. A Lagrangian particle model is used to initialise the Eulerian grid model during the first phase of the release. The particle model is a far simpler one than implemented in the PELLO model. In general the equation of mass-balance is solved;

$$\frac{\partial \rho c}{\partial t} = -\nabla V \rho c + \frac{\partial}{\partial z} \rho K_z \frac{\partial}{\partial z} c + Q + S + C(c,s)$$

ρ is the air density, c is the mixing ratio of the constituent, **V** the 3D wind vector, K_z the vertical turbulent exchange coefficient, Q the source term, S any sinks like dry and wet deposition, and C chemical transformation (may act as source or sink). Particle dynamics such as transformation between different particle sizes is not yet implemented. The above equation is solved in a discretesised form on the grid shown in Figure 5.1 (see Robertson et al., 1999, for details). The Lagrangian particle model is based on a similar mass-balance equation,

$$\rho \frac{dc}{dt} = \frac{\partial}{\partial z} \rho K_z \frac{\partial}{\partial z} c + Q + S$$

where the left hand side is described by Lagrangian particle transport including random displacement in the horizontal, while the right hand side is solved within an Eulerian framework. There is hence a transform involved, which converts particles to concentrations and vice versa. The Lagrangian particle model may therefor be regarded as a hybrid Lagrangian-Eulerian model itself. Chemical transformation is not included in the particle model.

Special attention has been paid to gravitational settling that is an important transport process for at least the largest particle fractions from a nuclear explosion. In the Lagrangian particle model this is treated explicitly. This is, however, more tricky to handle

within an Eulerian framework where the particles could, over one time-step, fall through a number of vertical layers and then violate the so called CFL-criteria for numerical stable solutions. One remedy to this is to use very short time-steps. We have though introduced a kind of slab-model, where a vertical column is assumed to "fall" with the speed of the falling particles.

In contrast to particle models like PELLO an Eulerian model can not handle a large spectrum of particle sizes. The particle cloud has to be subdivided into a set of particle fraction classes. Ten different fractions have been selected according to Table 5.1.

Table 5.1. Assumed particle size classes used in the MATCH model.

Particle size interval Radius (μm)	**Activity share (%)**	**Sedimentation velocity (cm/s)**	**Radius (μm) used for estimate of sink processes**
0 – 3	10	0.2	2.2
3 – 6.5	10	0.7	4.4
6.5 – 11.5	10	2.5	8.6
11.5 – 18.5	10	6.9	14.6
18.5 – 29	10	15.9	22.8
29 – 45	10	35.6	36.1
45 – 71	10	71.2	56.5
71 – 120	10	137.0	92.3
120 – 250	10	277.3	173.2
≥ 250	10	direct deposition	-

As indicated in Table 5.1, a nuclear weapon explosion gives rise to a wide particle size range. Particles larger than a few μm has a gravitational settling, a sedimentation velocity (v_s), which is increasing substantially for larger particles but rather constant with height in the atmosphere, see Table 5.1. The particle size distribution determines to a large extent the residence time in the atmosphere.

5.2.4 Determination of the friction velocity and boundary layer height

The formulation for friction velocity and boundary layer height is almost identical in PELLO and MATCH, as described in section 5.1.4 with the exception that in MATCH the friction velocity is set to its neutral value (see Robertson et al, 1999). Figure 5.3 shows an example of sensible heat flux and boundary layer height derived from the MATCH model.

5.2.5 Deposition

Dry deposition

In describing the total dry deposition for particles, we have separated sedimentation from turbulent transfer and surface processes of the dry deposition. We denote the total dry deposition velocity, v_d, and the sedimentation velocity due to gravitational settling, v_s, both positive downwards. The 'excess deposition velocity', (v_d-v_s), caused by the surface processes of dry deposition, is for these types of particles dominated by impaction to vegetation, ground and sea surfaces. Within and Eulerian framework the dry deposition is the lower boundary condition of vertical diffusion (Robertson et. al., 1999), which in principle is determined by

$$\frac{\partial \rho c}{\partial t} = -v_d \rho\, c\,.$$

We utilise prescribed reference values of the 'excess deposition velocity', $(v_d\text{-}v_s)$, which only has been estimated in a crude way since the total dry deposition is totally dominated by the sedimentation. We assume, for the time being, the following reference values, $(v_d\text{-}v_s)_{REF}$, at 1 m height above surface: forest 4, rural and urban 2 and sea 0 cm/s. In the MATCH model a correction for atmospheric stability in the lowest part of the atmosphere is included

$$(v_d\text{-}v_s) = \frac{(v_d\text{-}v_s)_{REF}}{1+(v_d\text{-}v_s)_{REF}/K_Z} \quad ,$$

where K_Z is the turbulent exchange coefficient for a ~50m layer close to the ground. This has however little influence on the results in this case, since the sedimentation dominates.

Wet Deposition

The wet deposition scheme is similar to particle size related scheme used in PELLO. The MATCH model utilises forecast precipitation amounts directly from the HIRLAM or ECMWF model. The following equations describes wet scavenging in MATCH,

$$\frac{\partial \rho c}{\partial t} = -\Lambda \rho c$$

where Λ is the washout coefficient given by,

$$\Lambda = \lambda(b_0 + b_1 r + b_2 r^2 + b_3 r^3)q \quad \text{for } r \leq 10\,\mu\text{m}$$
$$\Lambda = \lambda q \quad \text{for } r > 10\,\mu\text{m}$$

where q is the precipitation intensity (mm/h),

$\lambda = 2.78\cdot10^{-4}$,
$b_0 = -0.1483$, $b_1 = 3.220133\cdot10^{5}$, $b_2 = -3.00626\cdot10^{-4}$, and $b_3 = 9.34458\cdot10^{-4}$.

5.2.6 Time-step

The time-step is set to a fixed value of 6 minutes in the MATCH model, however, weather data given at every 3rd hour from the HIRLAM model are interpolated into one hour resolution.

5.3 Model comparisons with Chernobyl and ETEX-data

Both models have been applied to air pollution studies for compounds being transported only in the lower part of the troposphere. Data for those types of situations are more easily available and can be used for model verifications. That gives a possibility to investigate some basic formulations of the models, although no specific problems associated with the upper part of the troposphere and the stratosphere can be studied. Data from the Chernobyl accident and ETEX (European Tracer EXperiment) are

regarded as the most valuable data sets available for Europe. The comparisons of the models to the measured data sets are briefly described below.

5.3.1 PELLO model

Wet deposition calculated for the Chernobyl release shows a reasonably good agreement with measured values over Sweden. In Figure 5.4 the calculated wet deposition of Cs137 at 860501 06 UTC and the accumulated precipitation between 860428 06 and 860430 06 UTC, are shown. The precipitation rate, calculated as described above, is multiplied with a factor 2 in the calculations shown and the minimum precipitation rate allowed is 0.1 mm/h. These adjustments of model precipitation were done in order to obtain more realistic depositions fields. This need of tuning is mainly because of the crude precipitation calculations and point at the weakest part in the model. In the future precipitation rates from weather prediction models will be used, as soon as that kind of data becomes available. Comparisons can be made with observed precipitation and deposition of Cs137, as given in Figures 5.7.

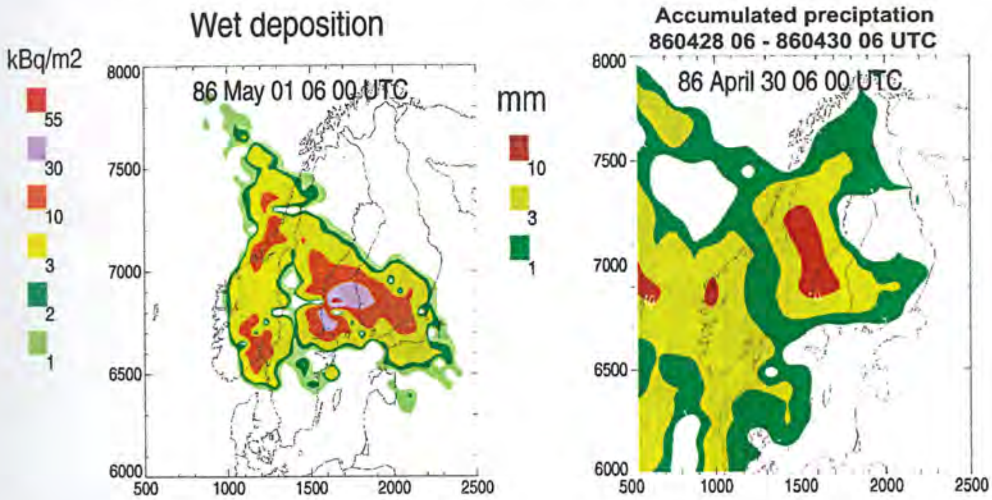

Figure 5.4 Results from the PELLO model: a) calculated wet deposition of Cs137 at 860501 06 UTC and b) calculated precipitation multiplied with a factor 2.

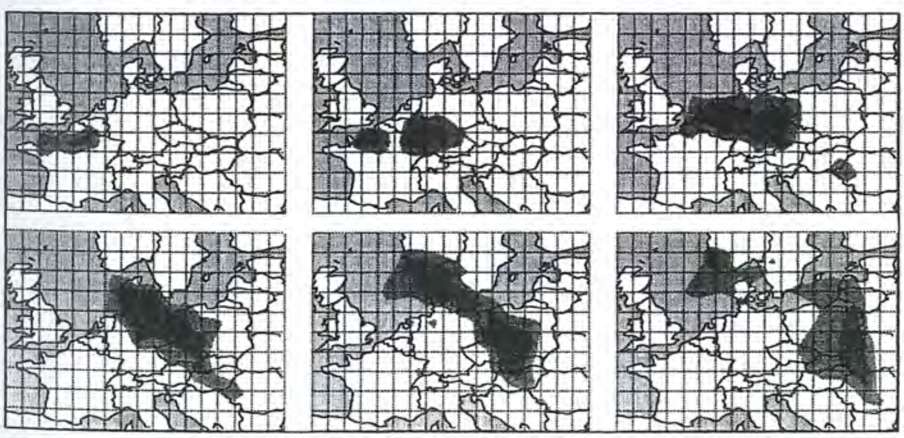

Figure 5.5. Estimation of the cloud position at 12, 24, 36, 48, 60 and 72 hours after the start of the release of the ETEX-experiment. The concentration levels (0.01 ; 0.1 ; 0.5 ng/m^3) are based on measured values. After Mosca et. al. (1997).

Comparisons with ETEX-data show good agreement, cf. Figures 5.5-5.6, which show measured and calculated concentrations respectively.

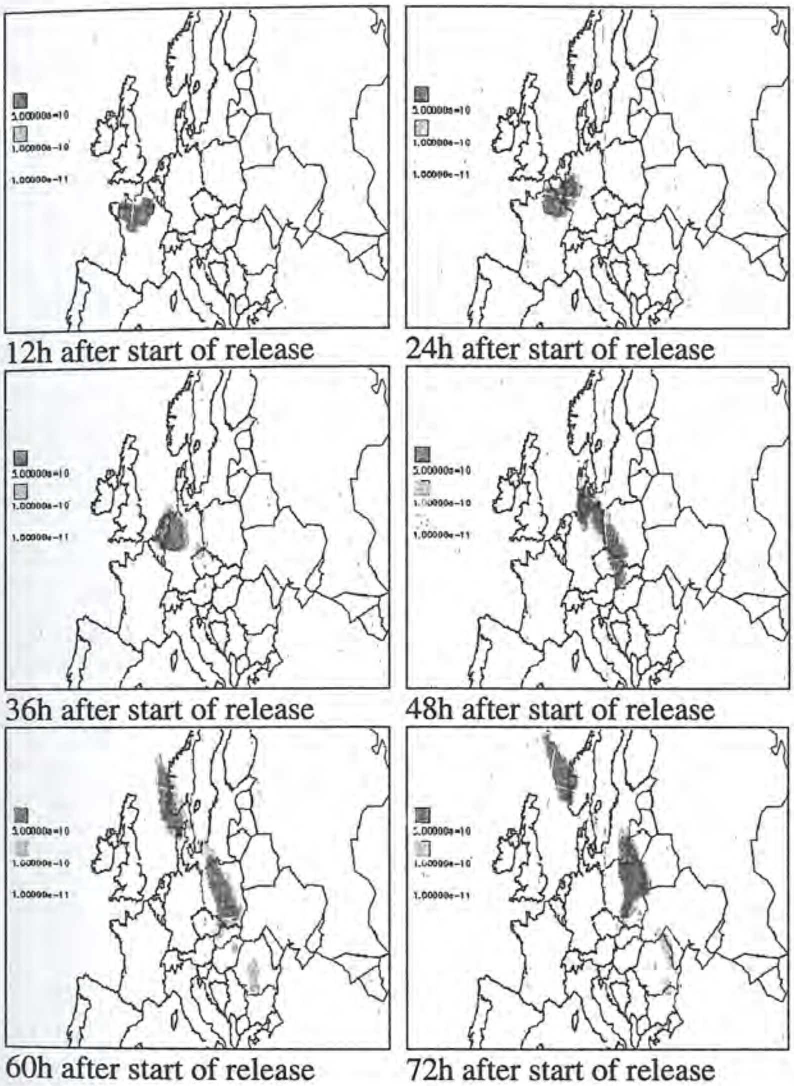

Figure 5.6. *Cloud positions for the ETEX-release calculated with Pello. Concentration levels are 0.01 ; 0.1 and 0.5 ng/m^3.*

5.3.2 MATCH model

Validation of the operational emergency response model, MATCH, at SMHI using data from the Chernobyl accident and ETEX have been presented by Langner et. al. (1998). In those validations the version of MATCH was designed for near surface releases, see Langner et.al. (1997).

Figure 5.7 shows the measured and simulated deposition of Cs-137 over Sweden associated with the Chernobyl accident. The general picture of the deposition is simulated very well, bearing in mind the rather coarse resolution of 50x50 km^2 grid cells. Comparing model results, total observed Cs-137 deposition and the accumulated precipitation during the four last days of April 1986, it becomes clear that wet scavenging was the dominating process for deposition over Sweden during the Chernobyl accident. It should be noted that observed precipitation fields were used as model input in this comparison. Using forecast precipitation does not give the same good agreement with observations of Cs-137 deposition (see Langner et al, 1998, for details).

Simulation of the ETEX experiment is shown in Figure 5.8 for four different times of the experiment. Measurements are marked with circles and coloured in the same way as the simulated cloud. MATCH obtained a high ranking in the ETEX comparisons with all available international models, Mosca et.al. (1998).

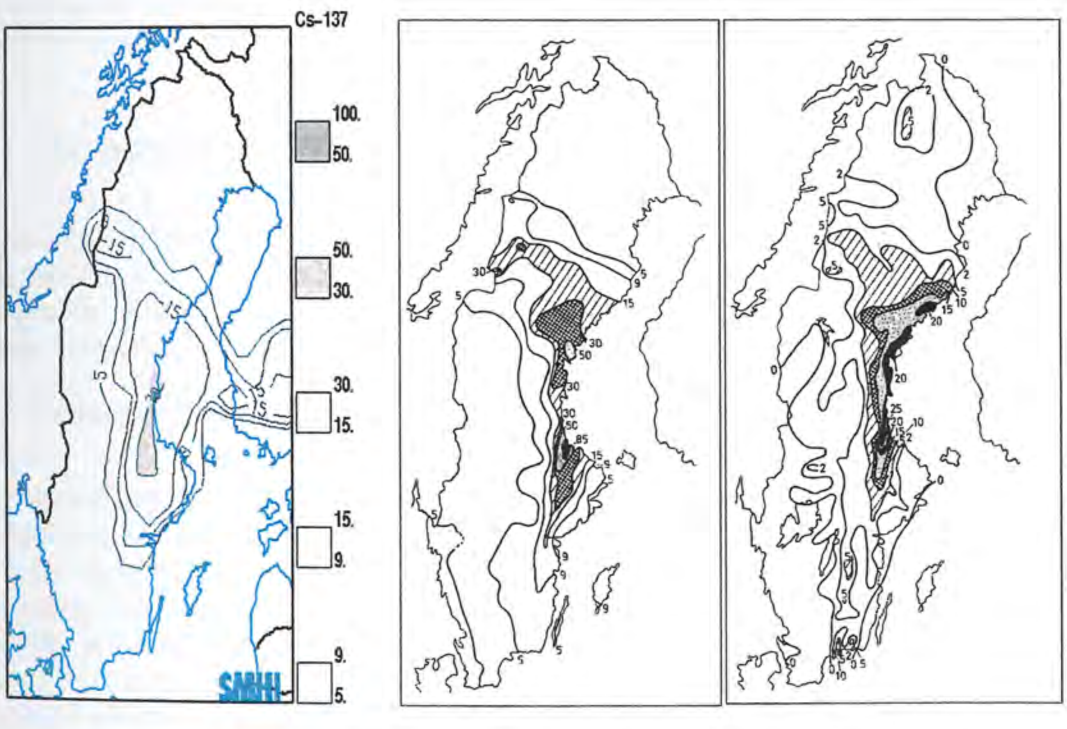

Figure 5.7. Left) MATCH simulated wet deposition of Cs-137 from the Chernobyl accident (kBq/m², April 26 06 UTC - May 01 06 UTC, 1986), middle) measured deposition of Cs-137 (kBq/m², May 1986) and right) measured accumulated precipitation (mm, April 28 UTC – May 01 06 UTC, 1986).

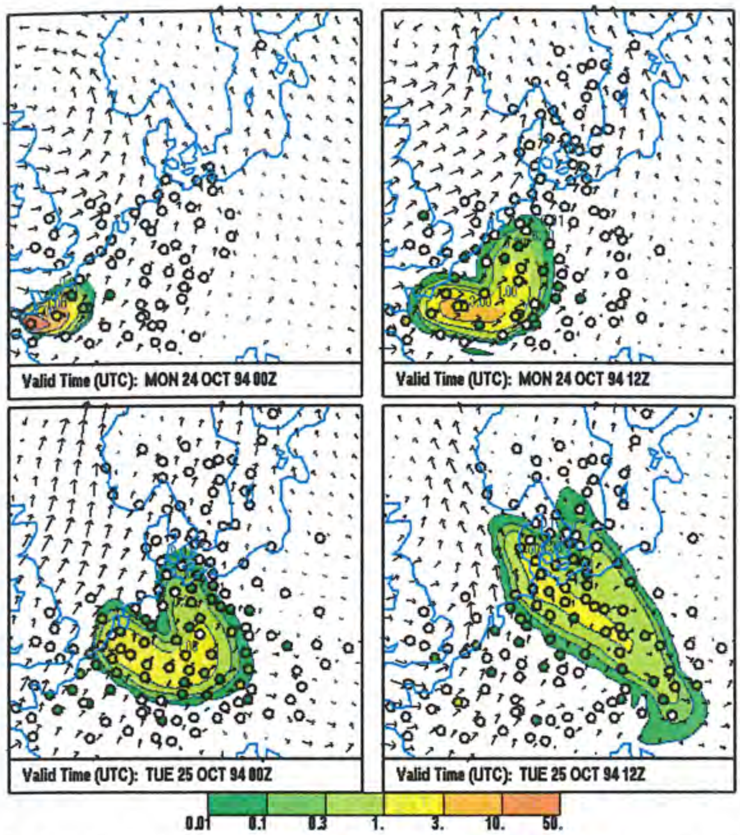

Figure 5.8. Simulation and measurements from the ETEX experiment at four different times of the experiment (corresponding to 8h, 20h, 32h and 44h after first release). Measurements are marked with circles and coloured with the same legend as the simulated cloud. Empty circles denote zero-measurements.

6 Results for nuclear weapon simulations

Results for model applications concerning the transport and deposition of radioactive contaminants from nuclear weapon explosions are presented partly as a comparison between the PELLO and MATCH models, partly as an illustration of how the two models were used in the national exercise Lotta.

6.1 Weather situation

The calculations for the model comparison as well as the Lotta exercise were based on weather data for the period May 13^{th} – 15^{th}1997. In Figure 6.1 some surface weather maps are shown. The situation was characterised by a low-pressure region over the Norwegian Sea and a weak high-pressure region over the Baltic Sea resulting in southerly or southwesterly winds over Scandinavia. From the weather maps it is also obvious that the precipitation over Sweden was quite small and consequently the wet deposition should not be expected to dominate the deposition pattern.

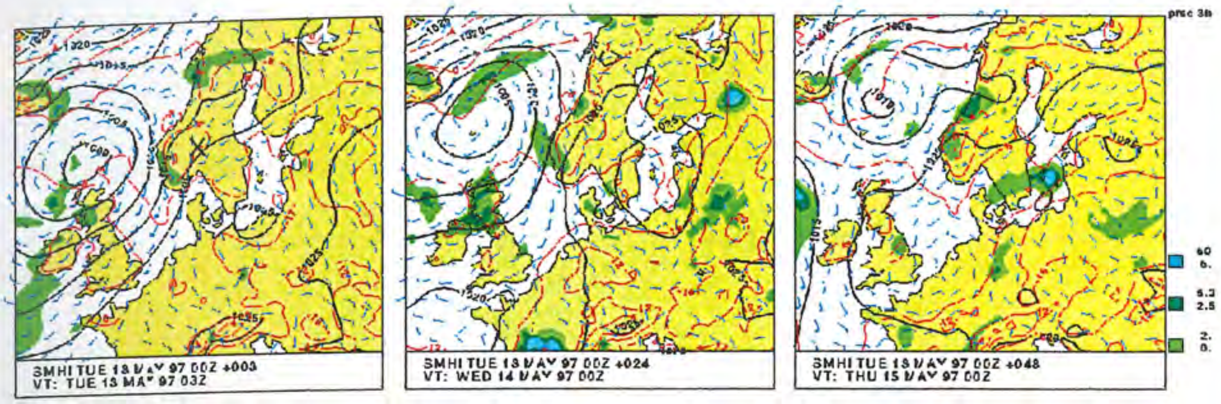

Figure 6.1 Weather maps for the studied period. HIRLAM forecasts (+3h, +24h and +48h) valid at May 13th 1997 03 UTC, May 14th 1997 00 UTC and May 15th 1997 00 UTC. The explosion point is marked with X on the map for May 13th 1997 03 UTC.

6.2 Comparison between the PELLO and MATCH models

The main difference between the SMHI model (MATCH) and the FOA model (PELLO) is that the former is based on an Eulerian formulation while the latter is based on a Lagrangian. In short this means that in the MATCH model, for each time-step, the concentration is calculated in grid boxes as a result from the net-transport due to 3-dimensional advection, sedimentation, dispersion and sink processes for each box. In the PELLO model the release is represented with a number of model particles which are given the speed of the mean wind plus a stochastic turbulent one. The number of model particles are then, at certain chosen times, counted in arbitrarily large grid boxes in order determine the concentration field. One advantage with Eulerian models is that they are normally less computer demanding and less time consuming than the Lagrangian ones, especially if a very large amount of particles are needed to describe the studied case and when atmospheric chemistry processes are included. In this case, the Eulerian MATCH model also has the advantage of already being in operational use at SMHI for the national emergency preparedness for nuclear reactor accidents. An important advantage with Lagrangian models is that it is possible to assign certain features to each model particle besides the amount of activity it carries, e.g. a radius and a settling velocity. In this way it is quite straightforward to describe a release with a size distribution.

In order to make a fare comparison both models have been run with the same weather data (HIRLAM forecast data) and for the same release scenarios (100 kt and 1 Mt). Location and explosion time for both cases were assumed to be 60°36' N, 11°0' E at May 13th 1997 at 00 UTC.

6.2.1 100 kt sceanrio

In Figure 6.2-6.6 the geographical distribution of the radioactive cloud in the near ground air and of the ground contamination are depicted. Results for the PELLO and the MATCH models are compared.

The contours for concentration in near ground air in Figures 6.2-6.6, right column, are given in kBq/m^3 at H+1, i.e. the *non-decayed* activity valid one hour after the detonation. This is the common way for radiologists to present activity originating from

nuclear weapons. The expected activity at a certain time after H+1 is often assumed to decay according to $A(t) = A(1) \cdot t^{-1.2}$, where A is the activity and t is the time in hours, after the explosion. The concentrations in the MATCH results refer to the lowest 60 m and in the PELLO for the lowest 500 m.

The ground contamination contours in Figures 6.2-6.7, left column, depict the dose rate at H+1 in mGy/h, i.e. the gamma radiation absorbed by an unsheltered person standing for one hour on the contaminated ground. Also here non-decayed values are commonly used.

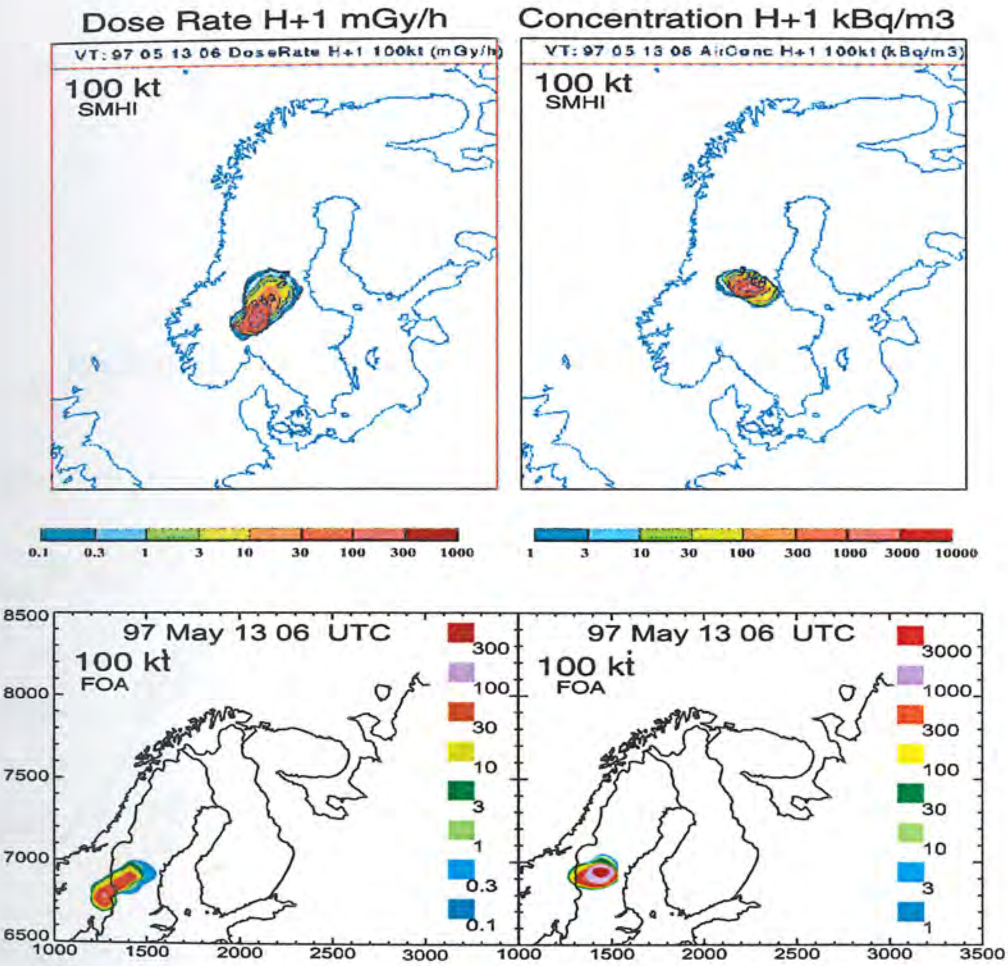

Figure 6.2 Explosive yield = 100 kt. The geographical distribution of the ground contamination (to the left, given in dose rate H+1, mGy/h) and the near ground air concentration cloud (to the right, given in H+1, kBq/m3) 6 hours after explosion. MATCH (SMHI) results on top and PELLO (FOA) results at the bottom. Note that the colours in the MATCH and PELLO results only agree approximately. For details about the H+1 notation and the contours, see text.

After 6 hours no obvious differences between the models have shown up.

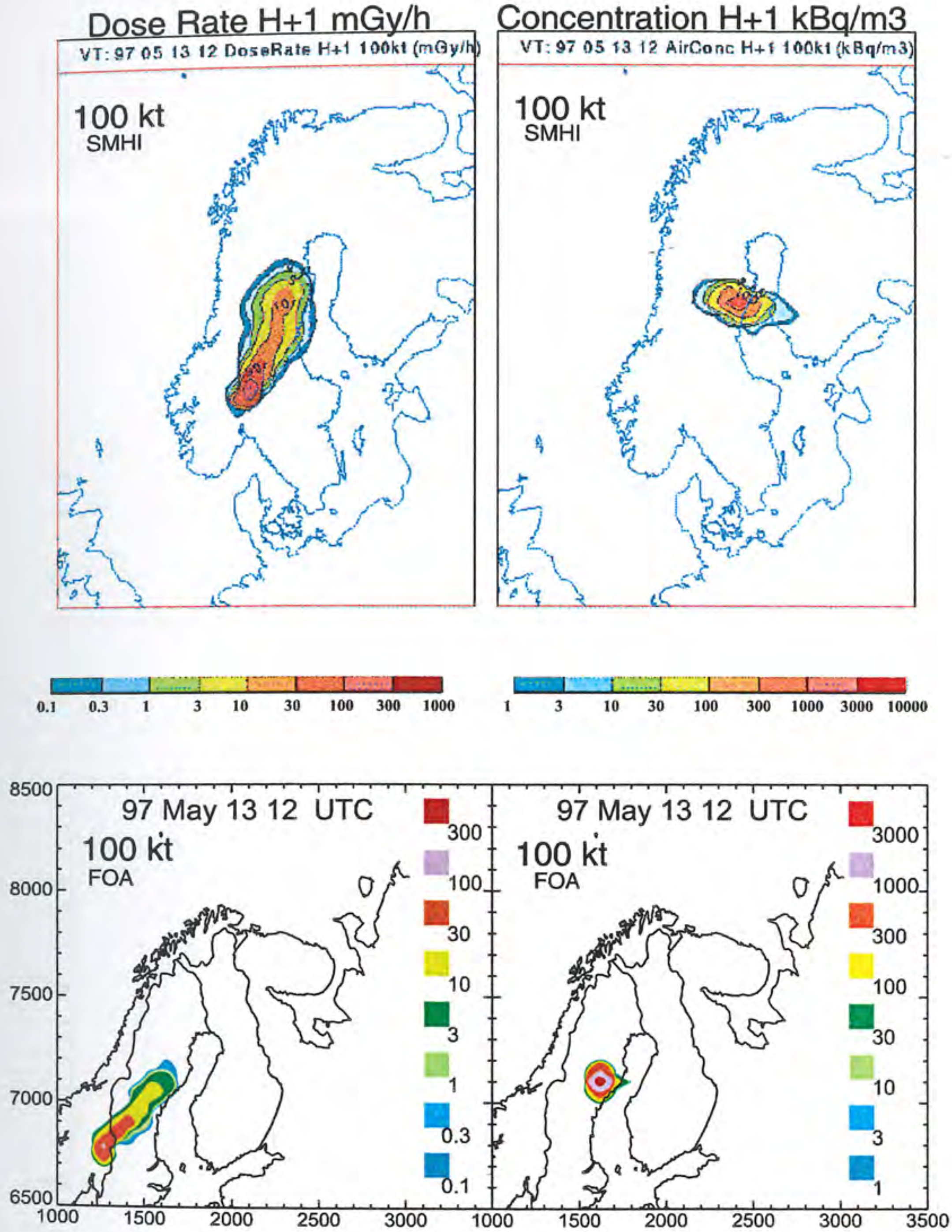

Figure 6.3. Same as Figure 6.2, but 12 hours after explosion.

After 12 hours the concentration in the near ground air cloud is less dispersed in the PELLO model and consequently higher concentrations are shown. It's notable that only the lateral dispersion differs. The predictions of the centre of the cloud agree very well for the two models. The ground contamination has the same magnitude although the MATCH prediction, in consequence with the larger lateral spread, is somewhat broader.

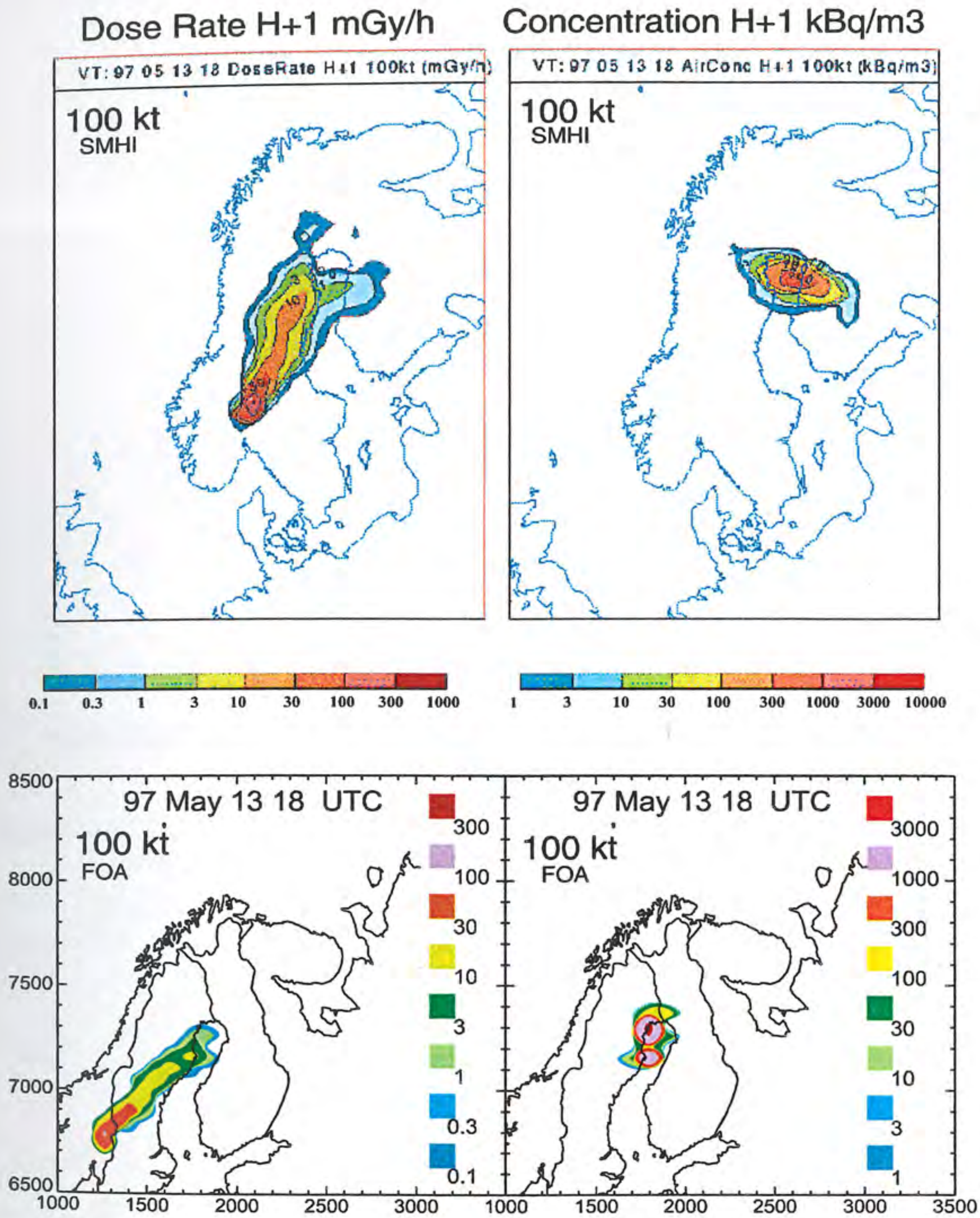

Figure 6.4. Same as Figure 6.2, but 18 hours after explosion.

After 18 hours the deviations between the models, which were seen after 12 hours, are even more accentuated. The MATCH near ground cloud and ground contamination do show a considerably larger lateral extension.

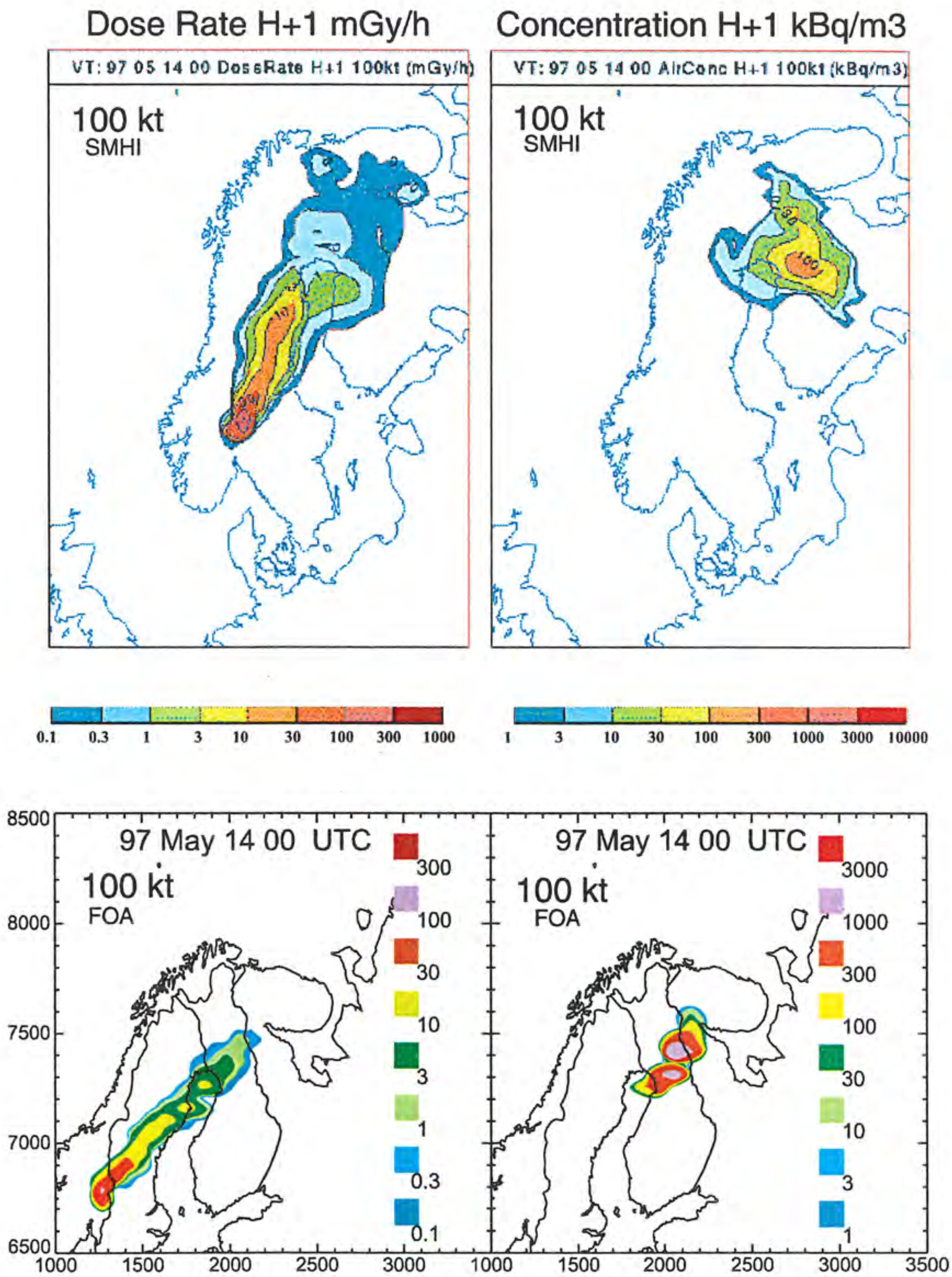

Figure 6.5. *Same as Figure 6.2, but 24 hours after explosion.*

After 24 hours the differences observed earlier have grown further. Areas of northern Finland and parts of the Kola Peninsula are reached in the MATCH predictions.

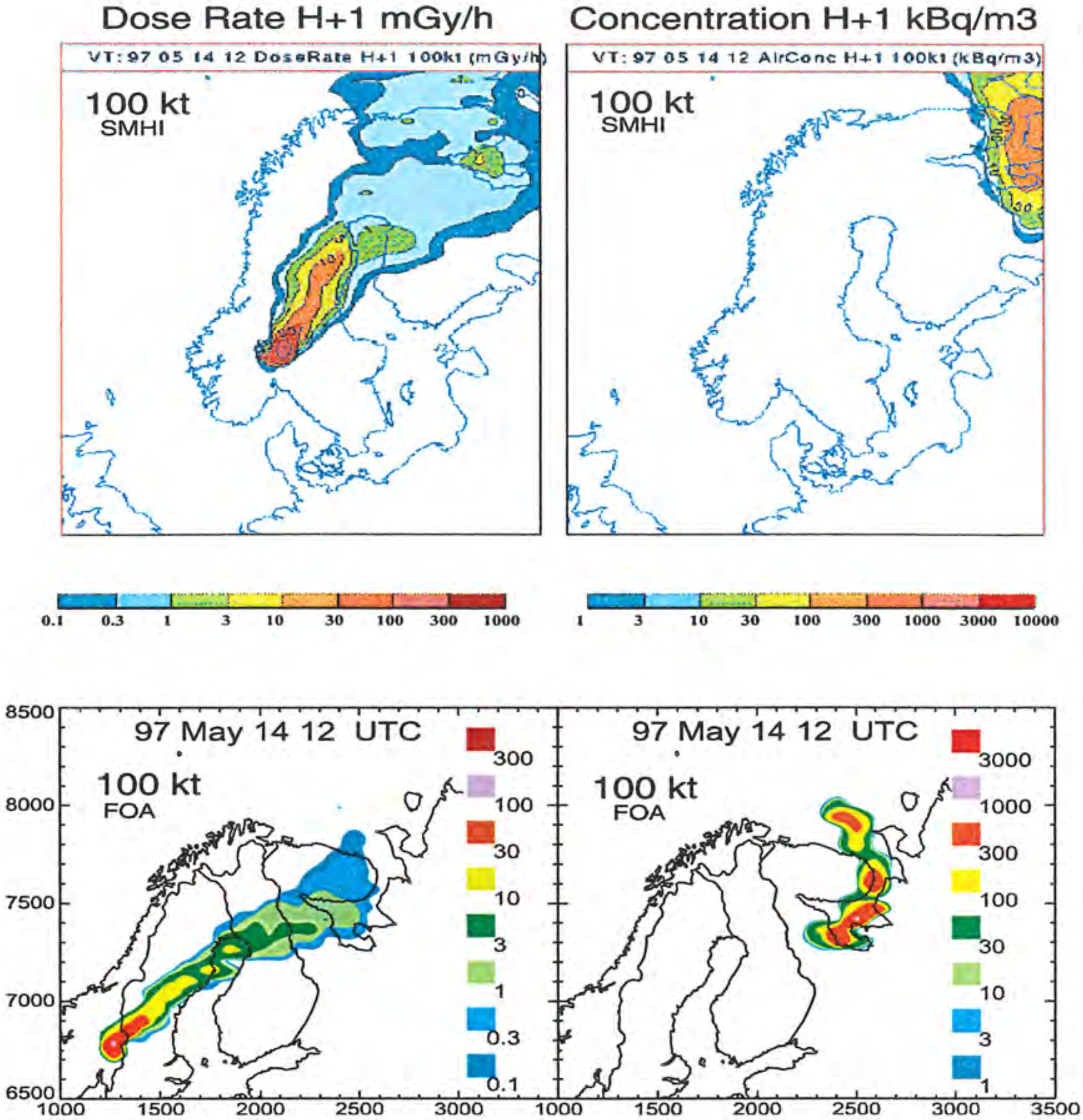

Figure 6.6. *Same as Figure 6.2, but 36 hours after explosion.*

After 36 hours the pattern from earlier still remains. The positions of the centre of the cloud do coincide reasonably well, but the lateral spread is much more pronounced in the MATCH prediction. Note that the more northerly extension of the cloud and the ground contamination produced with the MATCH model still can bee explained by a larger lateral spread, since the transport direction of the cloud gradually has become more easterly.

The more narrow distribution of the ground contamination in the PELLO results causes somewhat higher concentrations at ground level compared to MATCH.

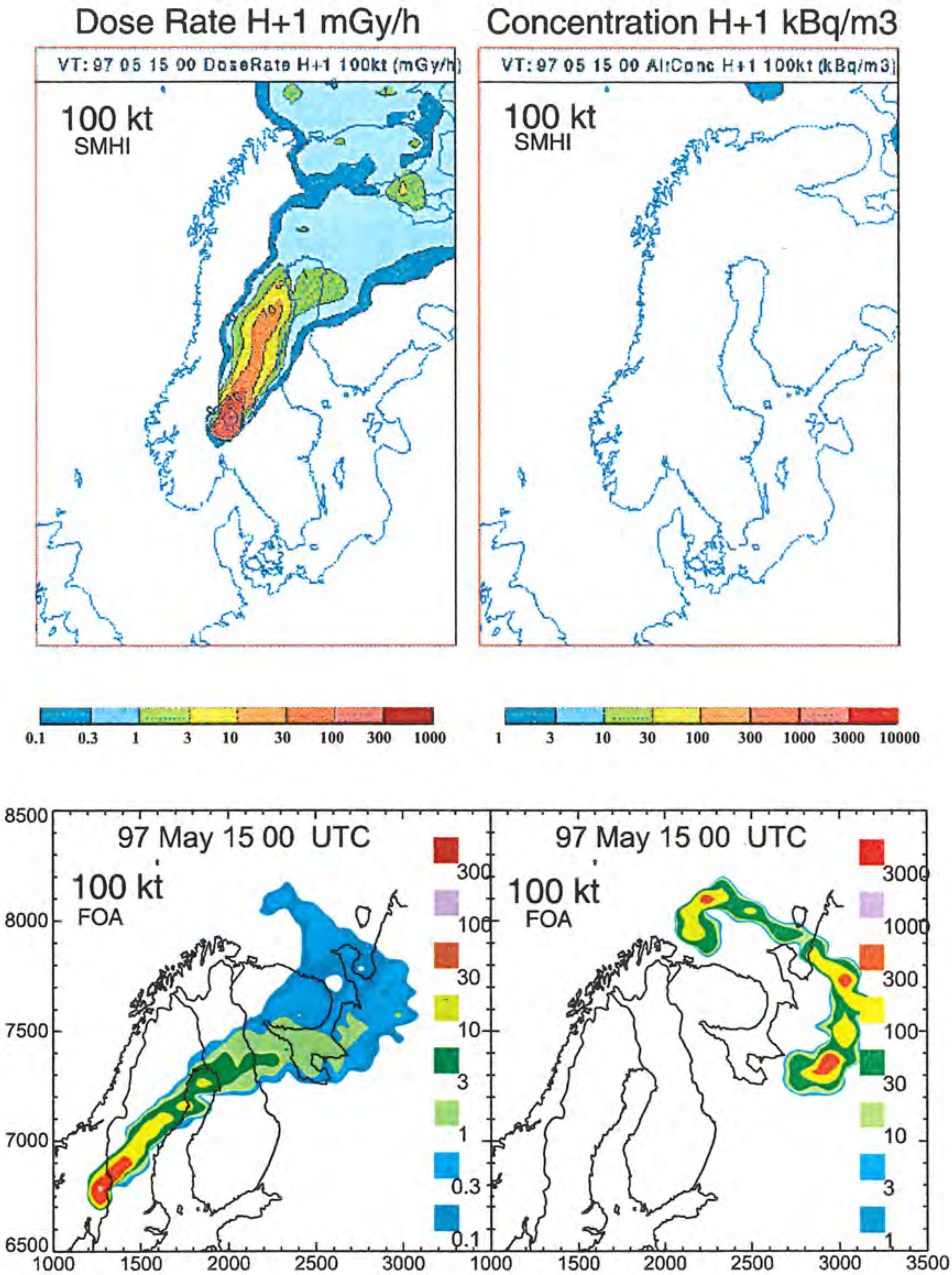

Figure 6.7. Same as Figure 6.2, but 48 hours after explosion.

After 48 hours a more widespread dose rate pattern, far from the source, is shown also for the PELLO model.

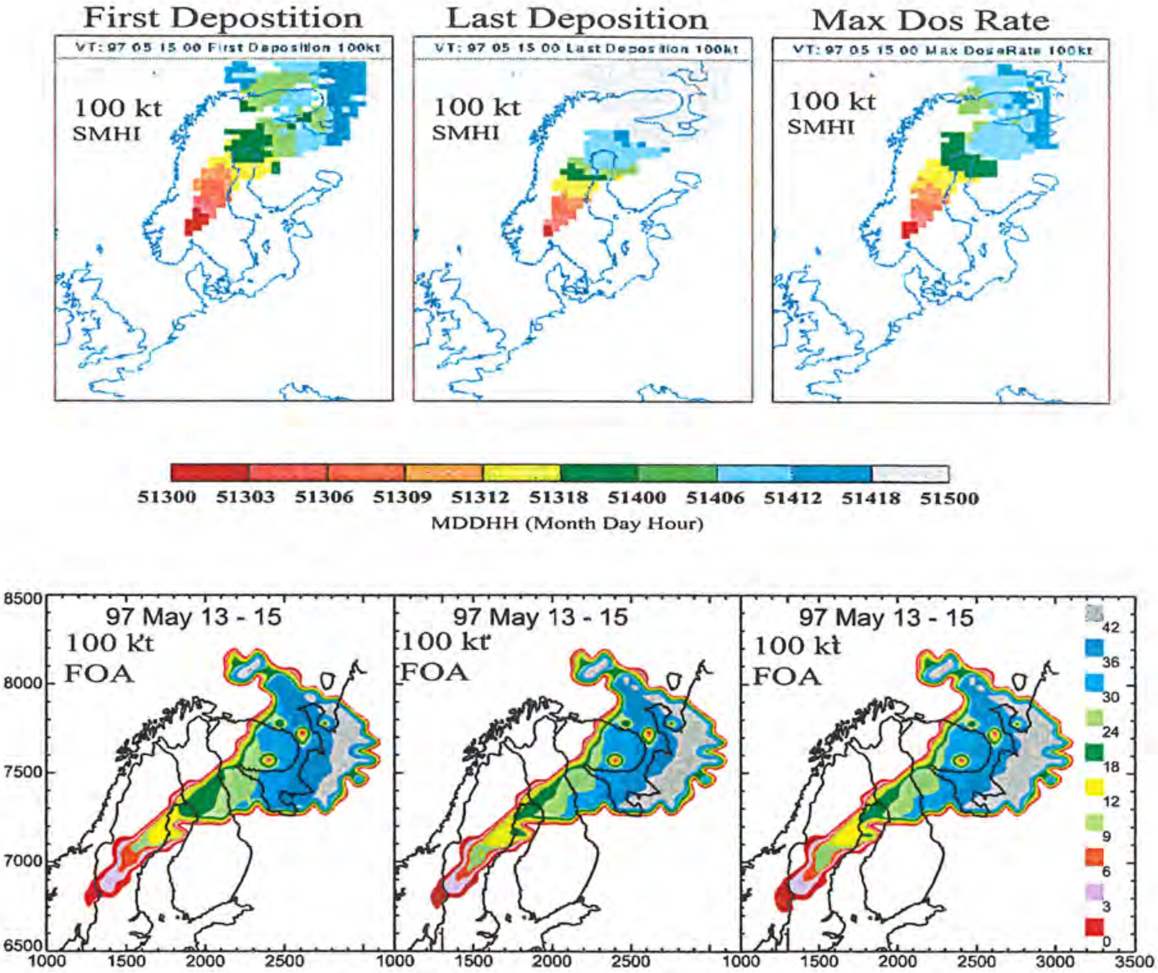

Figure 6.8. *Explosive yield = 100 kt. Maps showing a) first deposition time, b) last deposition time and c) time for maximum dose rate from the ground. MATCH (SMHI) predictions at the top and PELLO (FOA) results at the bottom. Note that in the MATCH figures date and time is used for the marking, while in the PELLO picture hours after the detonation is used. Note also that the colours don't coincide completely.*

The development in time for the ground contamination is depicted in Figure 6.8. The times for the first deposition, predicted with the two models are remarkably similar. Note that the "islands" on and beyond the Kola Peninsula in the PELLO picture indicating very early starting times are areas where the deposition never reached, cf. Figure 6.7. The misleading colours in these points are just consequences of problems with the software used when making contours. Also the pictures showing the time for maximum dose rate only show minor discrepancies between the models. The largest differences are found in the last deposition times where the PELLO results show considerably shorter deposition time. This feature can probably be explained by the smaller and more concentrated cloud (demonstrated in Figures 6.2-6.7) in the PELLO predictions.

6.2.2 1 Mt sceanrio

In Figures 6.9–6.13 the geographical distributions of the ground contamination and the radioactive clouds in the near ground air are depicted.

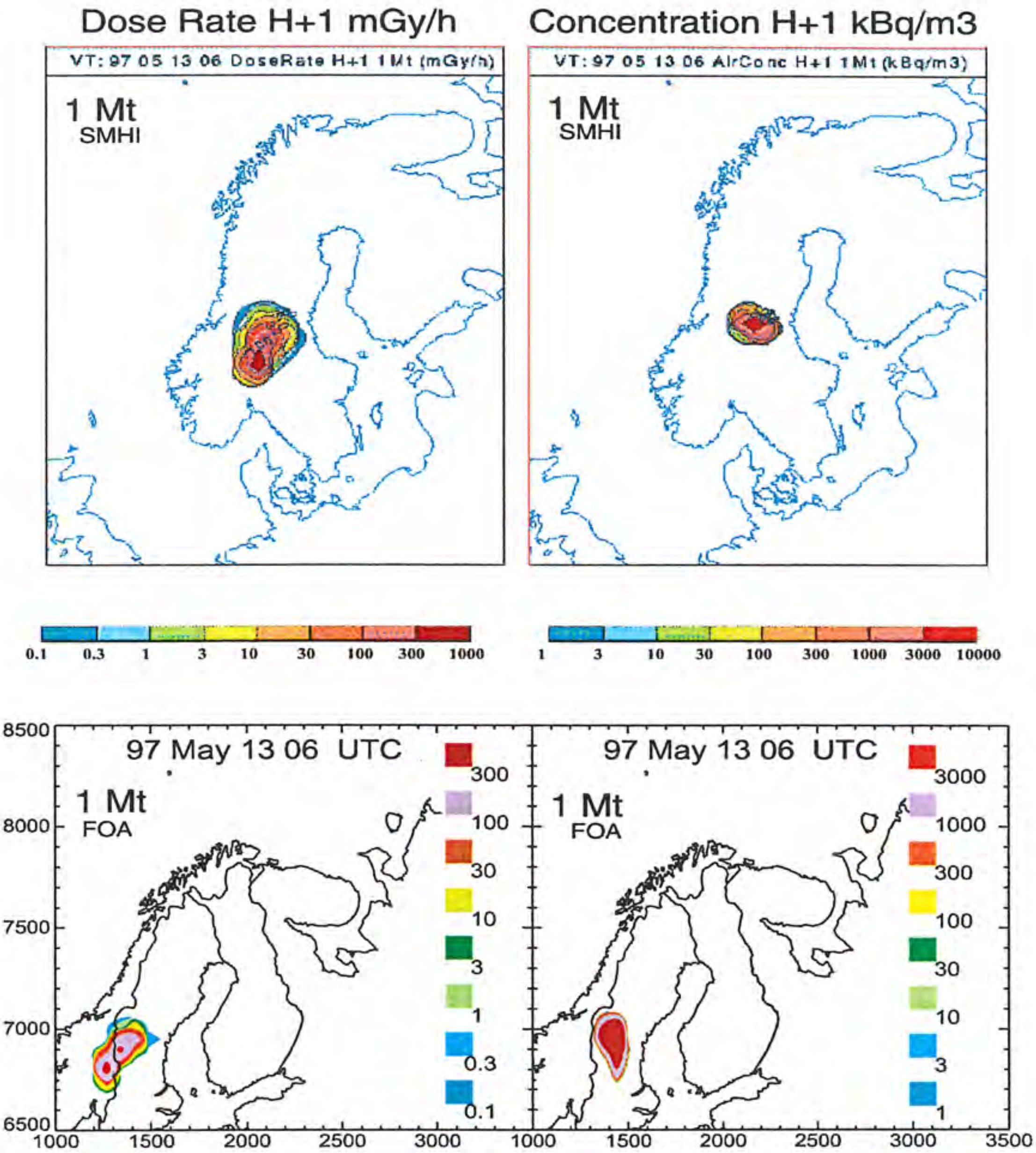

***Figure 6.9**. Explosive yield = 1 Mt. The geographical distribution of the ground contamination (to the left, given in dose rate H+1, mGy/h) and the near ground air concentration cloud (to the right, given in H+1, kBq/m3) 6 hours after explosion. MATCH (SMHI) results on top and PELLO (FOA) results at the bottom. Note that the colours in the MATCH and PELLO results only agree approximately. For details about the H+1 notation and the contours, see text.*

After 6 hours no significant differences between the model results can be seen.

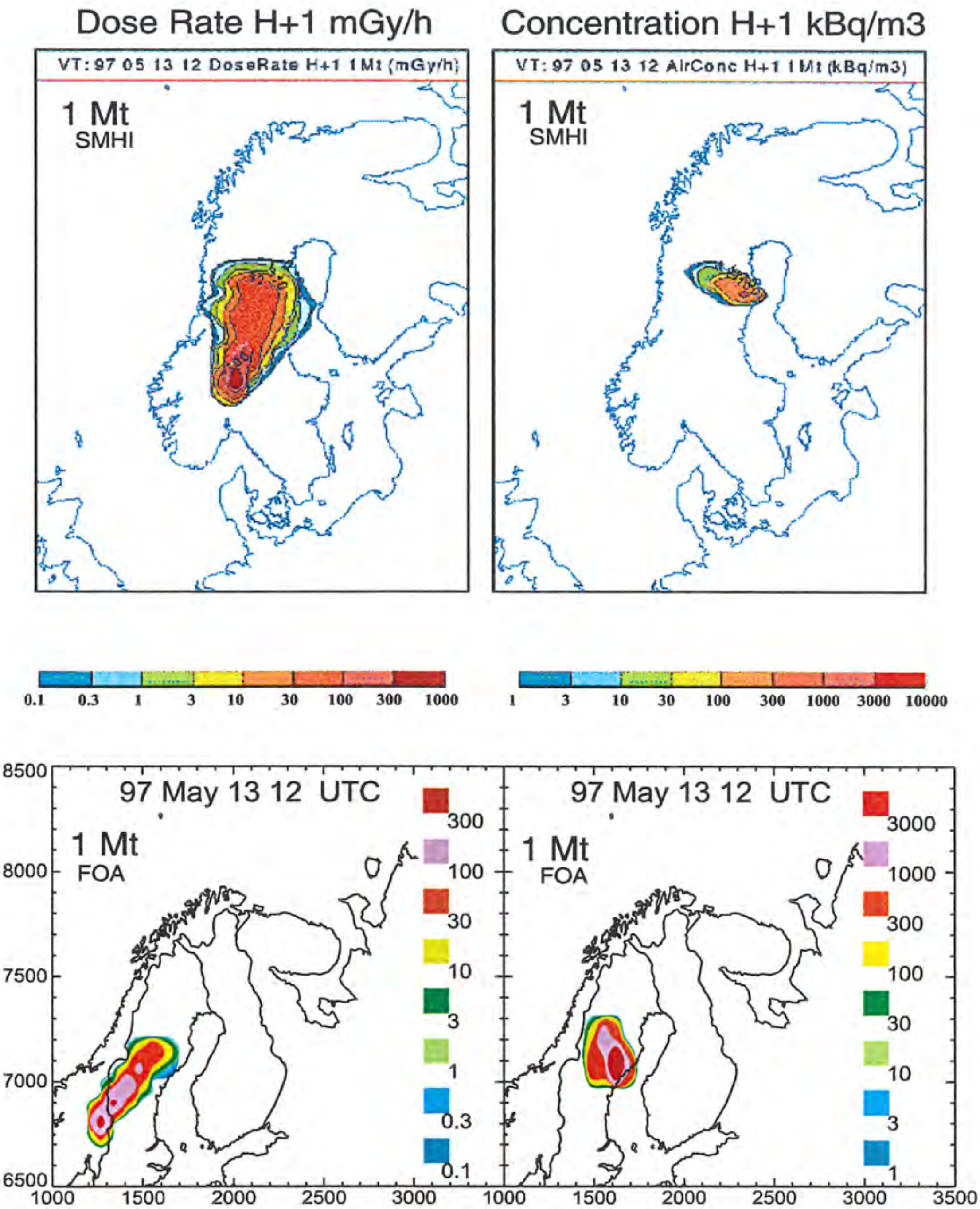

Figure 6.10*. Same as Figure 6.9, but 12 hours after explosion.*

After 12 hours the MATCH model predicts a broader and also somewhat more elongated ground contamination than does the PELLO model. However, the levels coincide rather well. The centres of the clouds are also quite close, although the "PELLO-cloud" has a higher concentration.

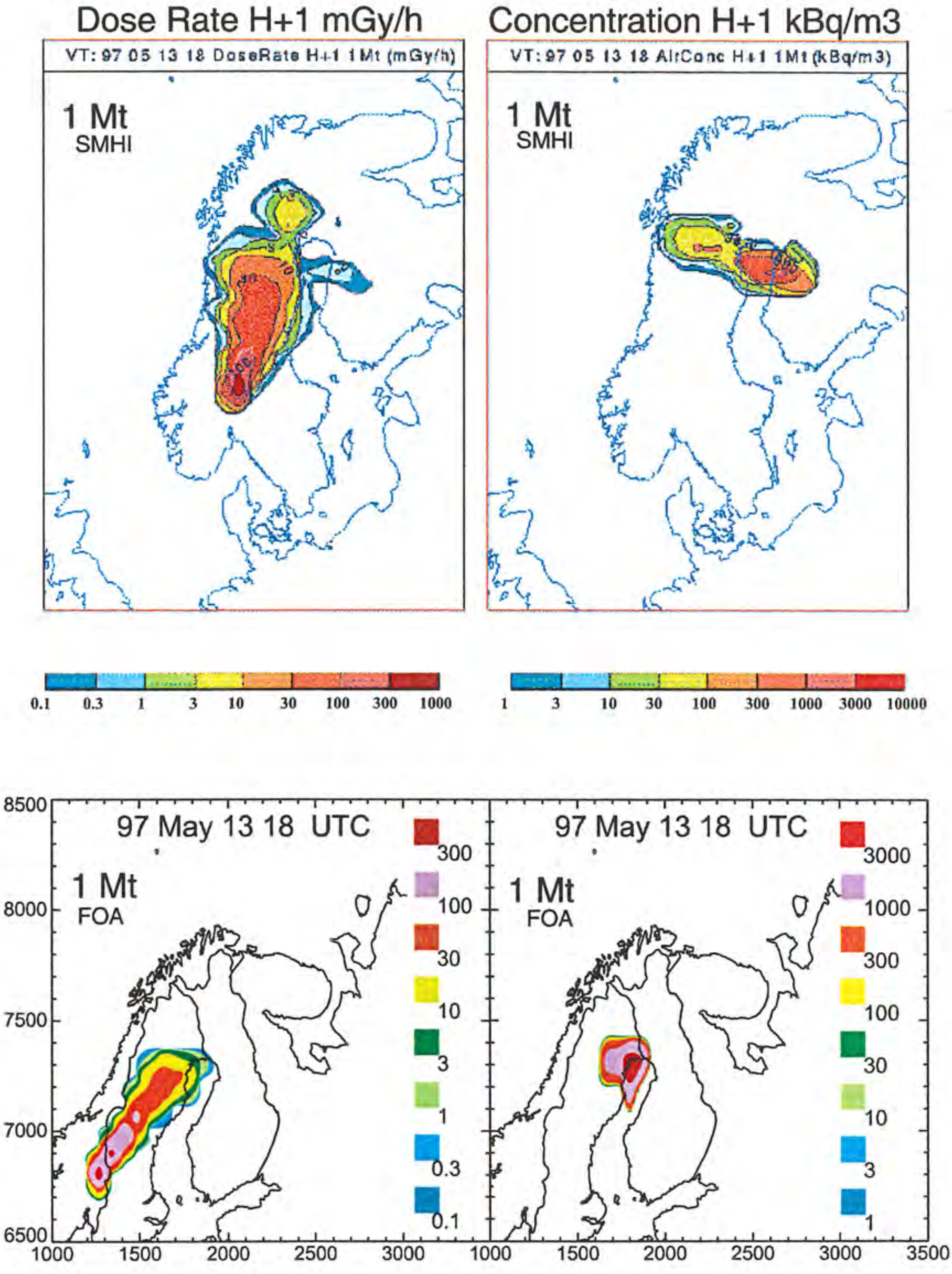

Figure 6.11. *Same as Figure 6.9, but 18 hours after explosion.*

Same tendencies as after 18 hours but the size of the "MATCH cloud" indicates a larger lateral spread as in the 100 kt case.

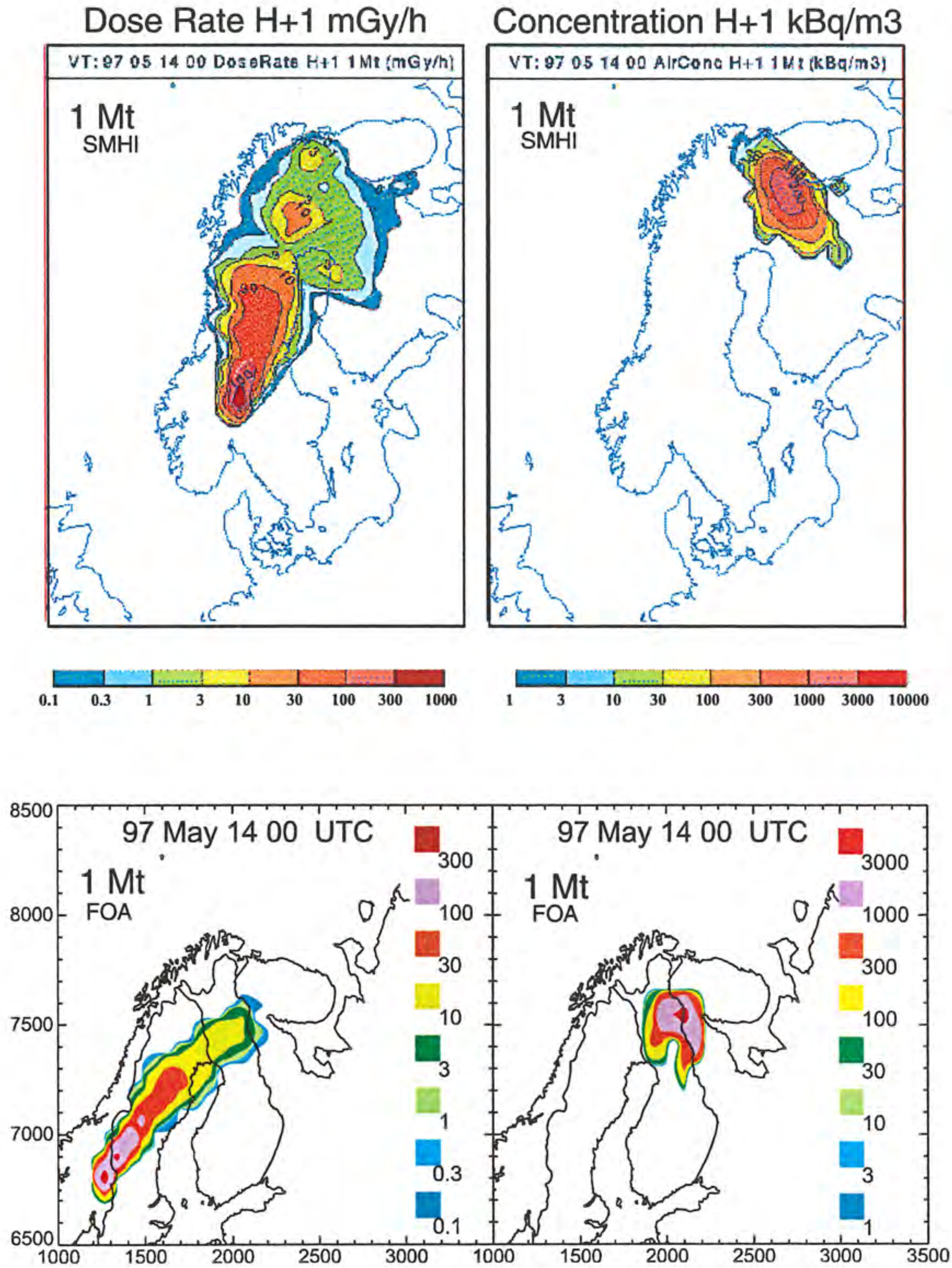

Figure 6.12 *Same as Figure 6.9, but 24 hours after explosion.*

Similar differences as after 18 hours.

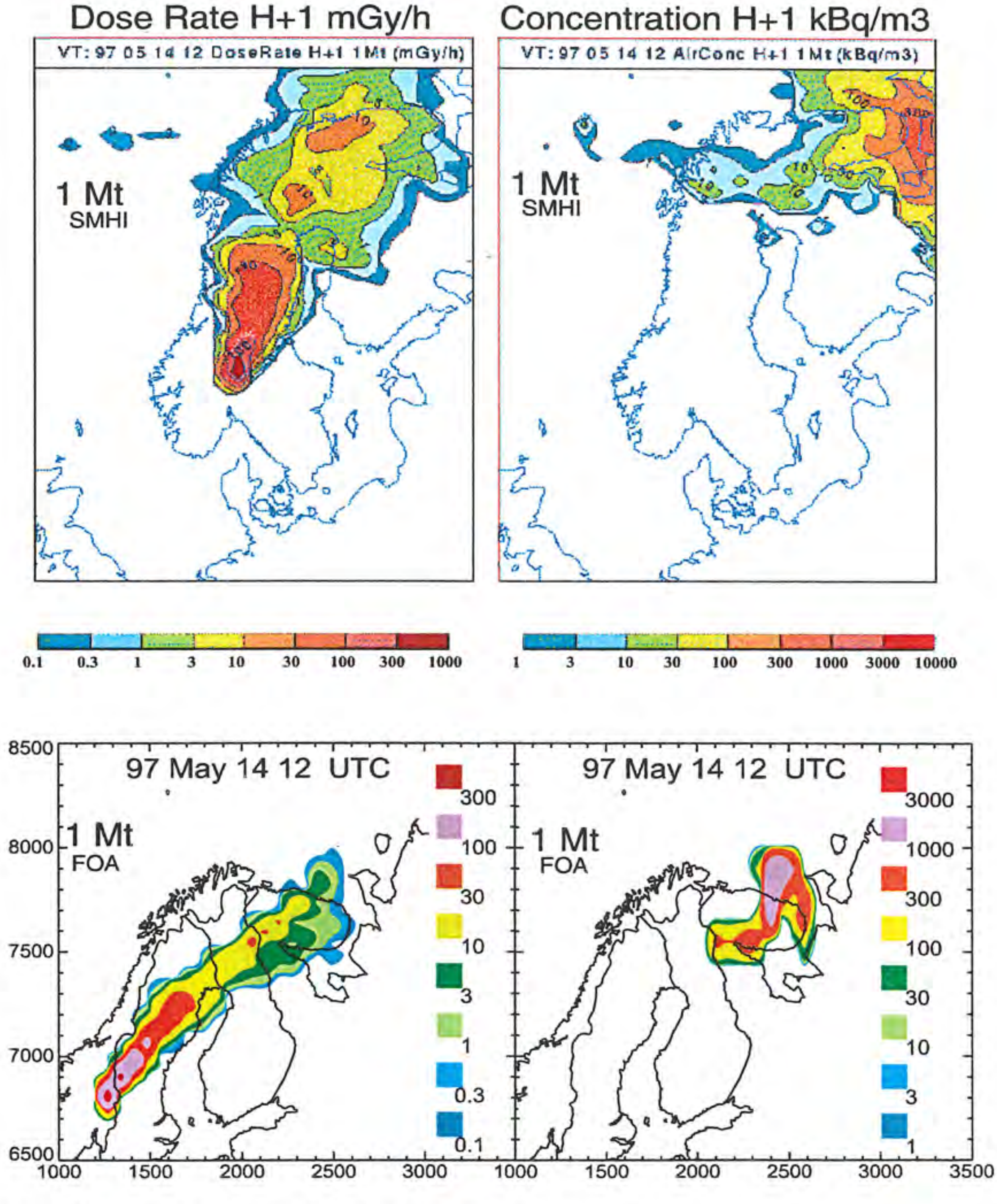

***Figure 6.13**. Same as Figure 6.9, but after 36 hours*

It's interesting to note from the MATCH (SMHI) run how radioactive particles suddenly appear far to the west of the earlier position of the cloud, and also much closer to the point of explosion. What is happening is that particles which have spent most of the time in the stratosphere, where the wind field might differ completely from that in at lower altitudes (troposphere), due to their settling velocity now reach altitudes close to ground. In the FOA run this phenomena has not yet shown up.

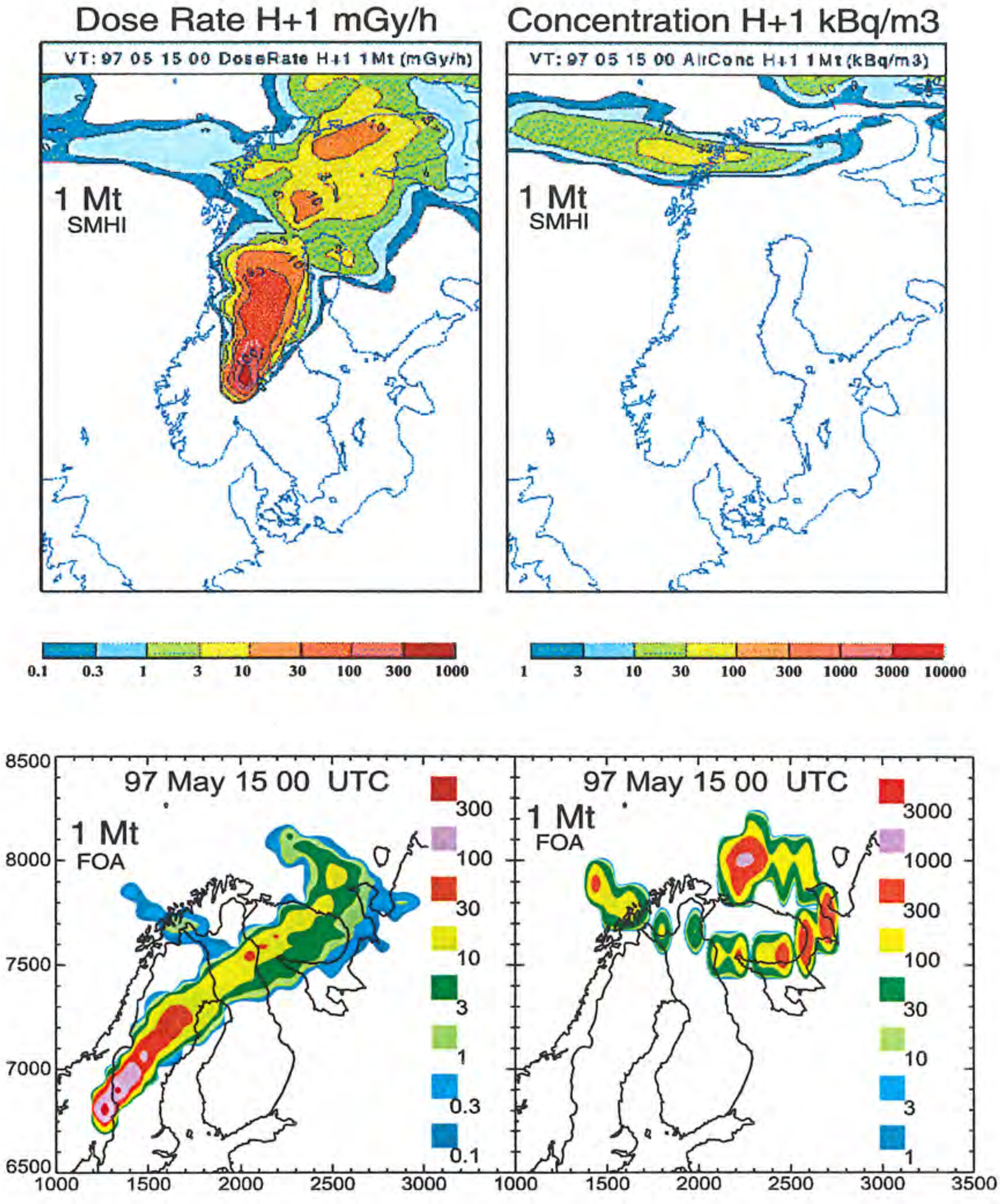

Figure 6.14*. Same as Figure 6.9, but 48 hours after explosion.*

After 48 hours also the PELLO (FOA) model produce the westward-situated branch of the cloud and of the ground contamination. Although the extensions are smaller than for the MATCH (SMHI) case the location and main features are very much the same. The maximum values both for the concentration and for the ground contamination at long distances, however, become higher in the PELLO results.

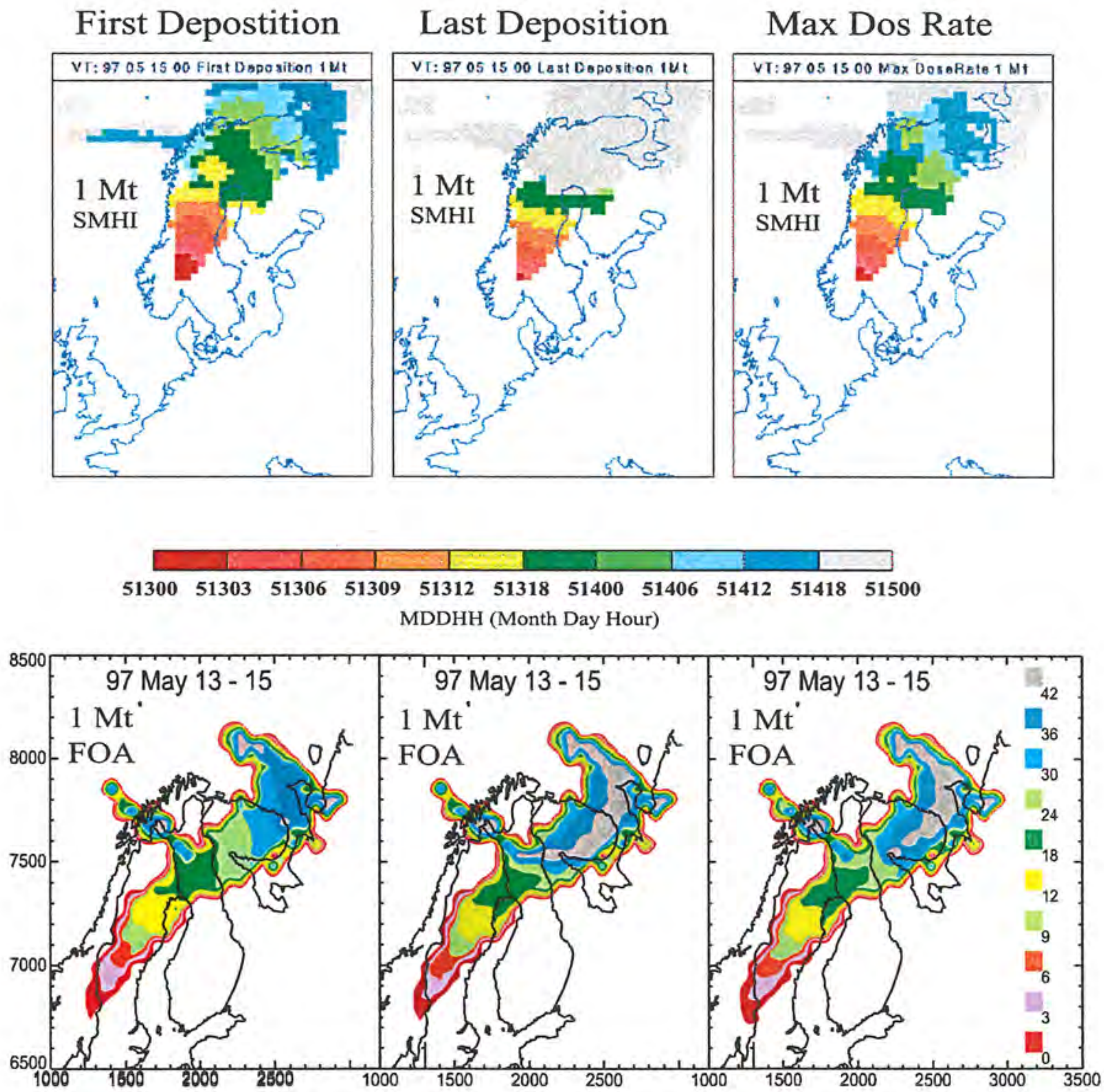

Figure 6.15. *Explosive yield = 1 Mt. Maps showing a) first deposition time, b) last deposition time and c) time for maximum dose rate from the ground. MATCH (SMHI) predictions at the top and PELLO (FOA) results at the bottom. Note that in the MATCH figures date and time is used for the marking, while in the PELLO picture hours after the detonation is used. Note also that the colours do not coincide completely.*

In Figure 6.15 basically the same features as in the 100 kt case (Fig. 6.8) appear. The first deposition times and times for maximum dose rate coincide rather well for the two models, while larger differences are found in the last deposition times where again the PELLO model brings the deposition to an end somewhat earlier.

6.2.3 Summary of comparisons

On the whole the MATCH model and the PELLO model produce very similar results in this comparison. The only obvious difference is the larger lateral dispersion in the MATCH model. The reason for this is not yet known, but requires a thorough investigation.

The good agreement between the two fundamentally different models, suggests that they are free from major errors. However, since the basic descriptions of emission processes and sink parameters are the same in both models, those parts have not been evaluated in this comparison.

7 Emergency preparedness system at SMHI

SMHI has for several years had an emergency response system (BAPS) for forecasts of atmospheric transport and deposition of radioactive substances in connection to nuclear reactor accidents. The purpose of the present project was to include a nuclear weapon module in the old BAPS-system. However, for technical reasons, it turned out that the old BAPS-system could not be used. A new system (JBAPS) has been developed, using a Java-based graphical user interface (GUI) and where the MATCH model is run on an Alpha server. The JBAPS system is described in the Appendix. The main part of the development of JBAPS has been financed outside this project.

References

Arkin, W., von Hippel, F. And Levi, B.:1982. *The Consequences of a "Limited" Nuclear War in East and West Germany.* Ambio XI, 167

Bridgeman, J.C.,Bigelow, W.S., 1982: *A New Fallout Prediction Model.* Health Phys., **43**, 205

Draxler, R.R., 1976: *Determination of atmospheric diffusion parameters.* Atmos. Env. **10**, 99-105

Klug W, Graziani G., Mosca S. Kroonenberg F., Archer G., Nodop K. & Stingele A.: 1995, *Real time long-range dispersion model evaluation - ETEX first experiment.* Draft report. JRC.

Lange, 1989: *Transferability of a Three-Dimensional Air Quality Model between two different Sites in Complex Terrain.* J. Appl. Meteorology, **28**, 7, 665-679

Langner, J., Robertson, L., Persson, C., & Ullerstig, A. (1997). *The operational emergency response model at the Swedish Meteorological and Hydrological Institute (SMHI).* In Proceedings from the ETEX symposium on long-range atmospheric transport, model verification and emergency response, Vienna 1997, K. Nodop (ed.), EUR 17346, European Commission.

Langner, J., Robertson, L., Persson, C., & Ullerstig, A. (1998). *Validation of the operational emergency response model at the Swedish Meteorological and Hydrological Institute using data from ETEX and the Chernobyl accident.* Atm. Env. Vol 32, No 24, 1998.

Lindqvist, J. 1999: *En stokastisk partikelmodell i ett ickemetriskt koordinatsystem. FOA.* FOA-report, FOA-R-99-01086-862--SE

Louis, J.F. 1986: *Research Manual 2, ECMWF Forecast Model, Adiabatic part.* ECMWF Research Department

Mosca, Graziani, Klug, Bellasio, Bianconi, 1997: *ATMES-II – Evaluation of Long-range Dispersion Models using 1st ETEX release data.* Joint Research Centre, Italy.

Nasstom, J.S., 1995: *Turbulence Parameterization for the Random Displacement Method (RDM) Version of ADPIC.* Lawrence Livermore National Laboratroy UCRL-ID-120965

Norment, H.G., 1979: *DELFIC: Department of Defenc Fallout Prediction System Vol I-Fundmentals.* DNA 5159F-1, Atmospheric Science Associates, Bedford, MA, AD-A088367

Näslund, E. & Holmström, H.: 1993, *Inclusion of a three-dimensional washout coefficient in ADPIC.* UCRL-ID 114054, Lawrence Livermore National Laboratory

Näslund, E. & Howard, C.R.: 1994, *A comparison between two stochastic diffusion models in a complex three-dimensional flow.* Boundary-Layer Meteorol. **67**,369-384

Näslund, Karlsson, 1995: *Dry Deposition in a Model for Stochasic Particle Dispersion.* Artikel i Air Pollution III: Volume 2 (Red: Power, Moussiopoulos, Brebbia), Computational Mechanichs Publications, England.

Näslund. E & Thaning, L.: 1991, *On the Settling Velocity in a Nonstationary Atmosphere.* Aerosol Science and Technology **14**, 257-256

Persson, C., Langner, J., & Robertson, L. (1994). MATCH*: A mesoscale atmospheric dispersion model and its application to air pollution assessments in Sweden.* In: Air Pollution and its Application, Vol. X. (Ed. E. Gryning.) Plenum Press, New York.

Peterson, K.,R.:1970. *An empirical model for estimating world wide deposition from atmospheric nuclear detonations.* Health Physics 18, 357-378

Robertson, L., Langner, J., & Engardt, M. (1999). *An Eulerian limited area transport model.* J. Appl. Met. Vol 38, pp 190-209, 1999.

Thaning L.: 1994, *Resulting ground contamination i Sweden after hypothetical releases of radioactive particles on the Kola peninsula.* Internt PM FOA

Thaning, L. & Näslund, E.: 1991, *A simulation of radiactive fallout using the MATHEW/ADPIC model.* FOA Report C40292-4.3

Zilitinkevich, Mironov, 1996: *A Multi-Limit Formulation for the Equilibrium Depth of a Stably Stratified Boundary Layer.* Boundary-Layer Meteorology **81**, 325-351.

Appendix

EMERGENCY PREPAREDNESS SYSTEM AT SMHI

Lennart Robertson, SMHI and Anders Rodrick, Mandator

An emergency response system for forecasts of atmospheric transport and deposition of radioactive substances has been developed and is now kept in 24h per day preparedness at SMHI. This system (JBaps), which is installed on an Digital Alpha workstation, is based on the atmospheric transport model MATCH and a graphical user interface. Three versions of the MATCH model are applied within the system; for emissions from nuclear reactors, for trajectory calculations and for emissions associated with nuclear weapons (see model presentation above). Duty forecasters in operational work are responsible for the 24h preparedness, while model experts can assist with some delay.

The graphical user interface is based on Java technology with a client/server approach that enables access by a web browser, which facilitates platform independent user access. So far access is only prepared for the internal Intranet at SMHI, but there is a potential for external Internet use in the future. The system design is schematically shown in Figure A.1. The client communicate with the server in two ways, via http protocol for visualisation of results and RMI (Java Remote Method Invocation) protocol for instructions from the client to the server to start model runs, invoke visualisation of results etc.

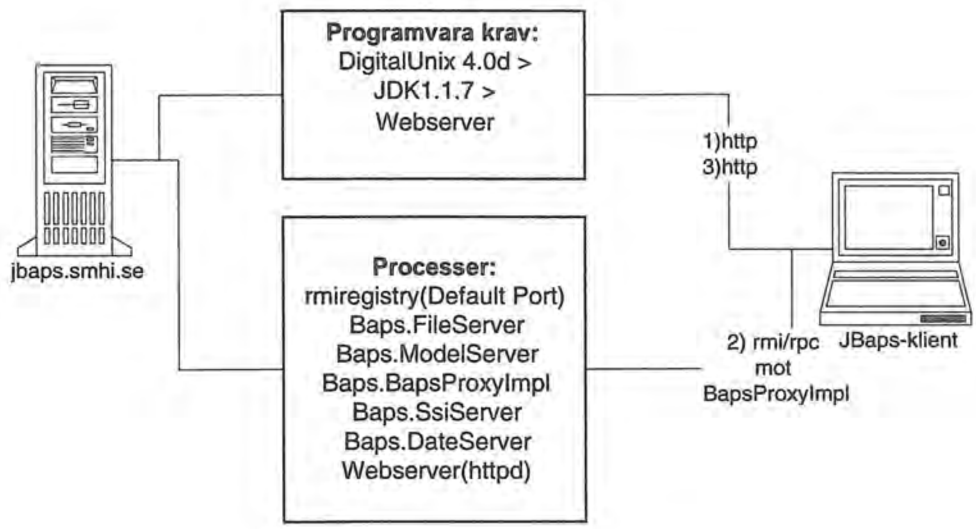

Figure A.1. Client/server design of JBaps. The client may be any platform like PC, Mac, Unix workstation etc., while the core system runs on a dedicated Digital Alpha workstation. The client communicate with the server over two paths, http protocol and Java RMI protocol.

The JBaps system is also supervised continuously at the computer control centre at SMHI where any disturbances in the system are notified and corrected. Figure A.2 shows the control panel for the JBaps system. Besides the Java based interactive access to JBaps, a number of operational model runs are performed. Those are mainly focused on accidental releases from nuclear power stations. All the Swedish reactors and most of the reactors around Sweden are covered by these runs. The objective is to have standard type of simulations already produced in case of any accidental release. The model simulations cover 48 hours ahead and are updated 4 times daily.

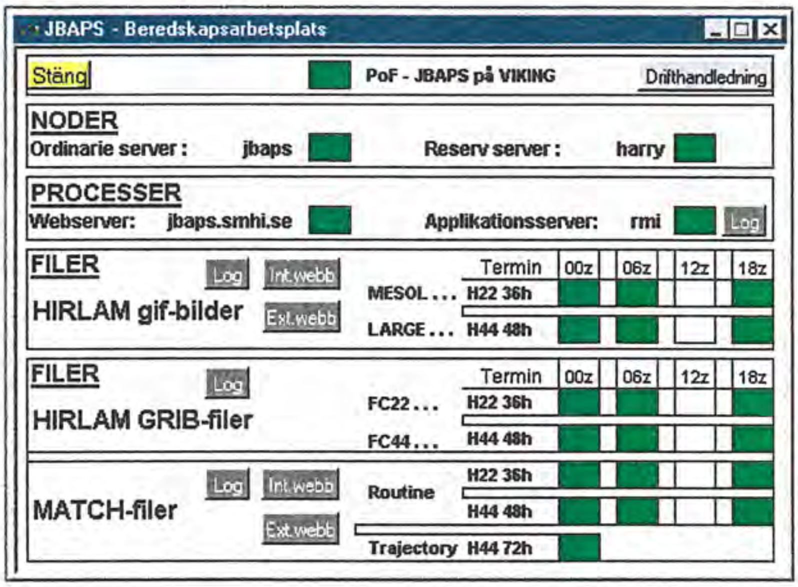

Figure A.2. *Control panel for supervision of the JBaps system at the computer control centre at SMHI (in Swedish). The figure shows a number alarm positions that could be activated, such as missing contact with computers, vital demon processes not running and result file production control.*

Access to JBaps for interactive use is made by a web-browser. Figure A.3 shows the first entry points the user will meet, a welcome page, a start button, and a start panel for model selection. From the welcome page (upper left panel in Figure A.4) it is possible to log on as forecast meteorologist (called JBaps PM) or as expert (called JBaps Expert). The JBaps PM interface is designed for as easy use as possible with just a few selections possible. The JBaps Expert interface is more elaborate aimed for a trained user, It is olny the Export user that could initiate sinulations for nuclear weapon events. The model selection panel (lower panel in Figure A.4) enables the Expert user to select between MATCH simulation for reactor events, trajectory calculations in order to trace contaminated air backwards/forwards or MATCH simulation for nuclear weapon events (the "Bomb" button in Figure A.4).

Figures A.4 to A.10 show the specific options for atmospheric dispersion simulations of nuclear weapon explosions.

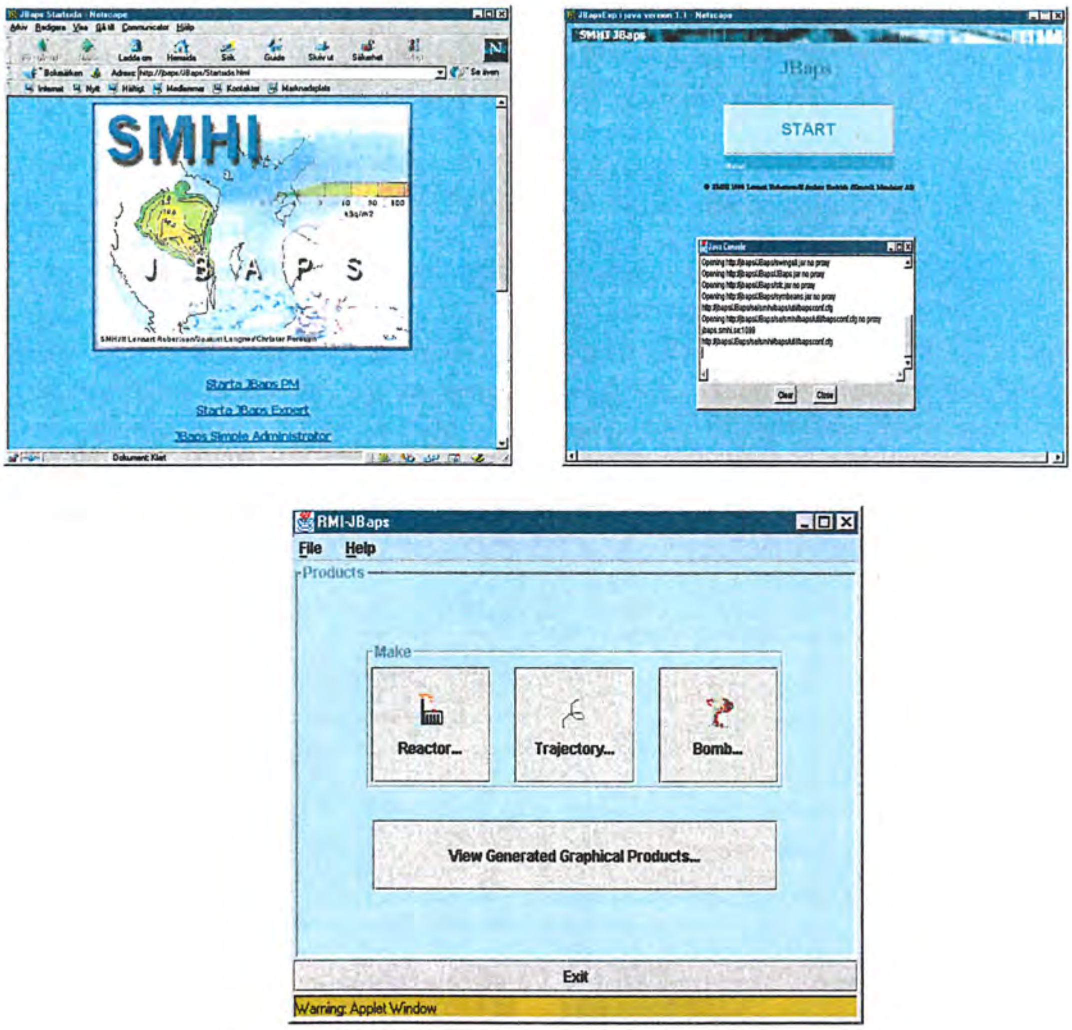

Figure A.3. *The first entry points for interactive access to JBaps by using a web-browser, the welcome page (upper left), start button (upper right), and the entry panel for model selection (lower panel). The upper right panel also shows the Java consol for messages about the appearance of the Java application.*

Figure A.4 shows the main panel for setting up MATCH for an nuclear weapon event. The user is requested to select model area, weather data, source point location, explosion yield, and start date of release. It is possible to list the available weather data, by the "List" option in the upper left corner of Figure A.4. A result of such a listing is shown if Figure A.5. The source location may be selected among predefined entries or by a "User Defined" option (Figure A.5). The location is determined by the longitude and latitude of the explosion while the vertical positions is predefined for each explosion yield.

When all is selected in the menu the model is started with pressing 'Go' button. A progress bar will then show up telling about the estimated time left for the simulation run, see Figure A.6, and a feedback panel giving product generation information, see Figure A.7. Products generated could be visualised by a click on the item, which will turn up in a separate web-browser window. An example of one of the products is shown in Figure A.8.

The feedback window has an optional button for sending the results to a web page for FOA accessible only for those authorised ("Send to FOA" button in Figure A.7).

Besides the various model options shown in Figure A.3, there is also an option for viewing results already produced. Figure A.9 shows the selection panel for viewing model results. It is then possible to in the first place select among model types (Reactor, Trajectory and Bomb), and secondly various product for each simulation run.

Finally, Figure A.10 shows the web page accessible from outside SMHI aimed for ÖCB, FOA and others that are authorised. Besides the simulation runs from MATCH, actual weather data such as satellite images and radar images, and numerical weather forecasts, are available.

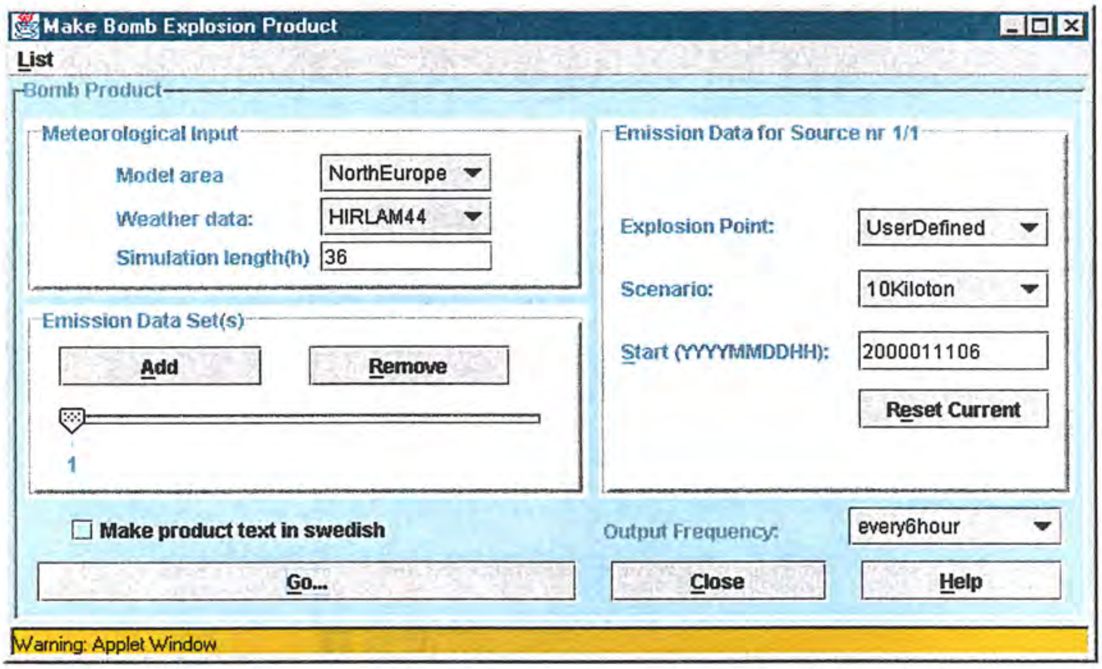

Figure A.4. Main interface to the bomb version of the MATCH model. The panel provides options for model area, weather data, source location , explosion yield, and time of the release. It is possible to enter a number of release points. The "List" option indicates possibility to list available meteorological data (see Figure A.5).

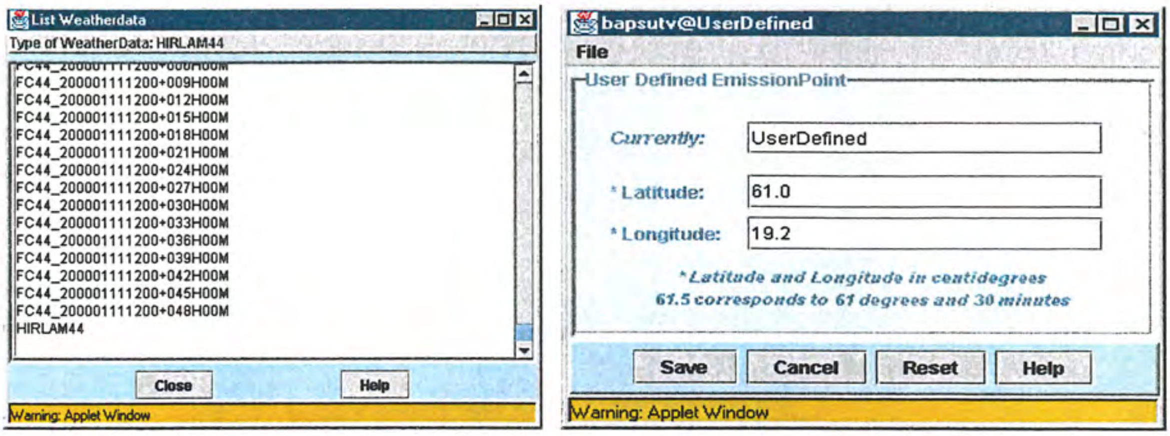

Figure A.5. *Optional pop-up panels for listing of available weather data (left) and for user defined source location (right). The shown listing refers to HIRLAM data with 44 km resolution (FC44). The user defined source location is determined by the latitude and longitude of the explosion. The vertical position is predefined for each explosion yield.*

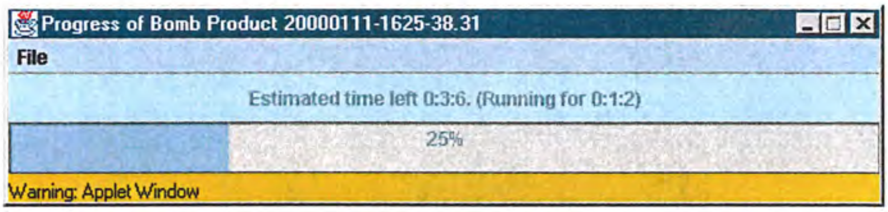

Figure A.6. *Running time information for the MATCH model.*

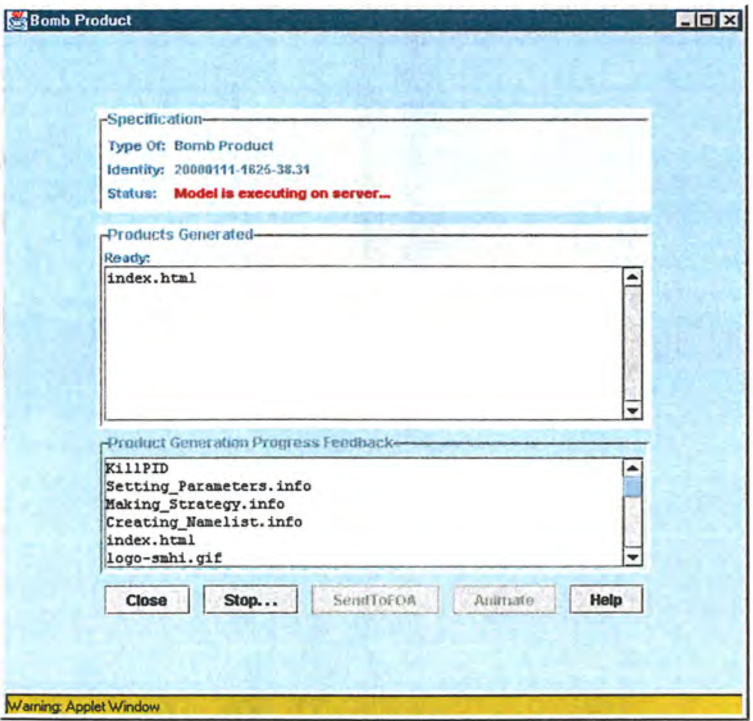

Figure A.7. *Product generation information and progress feedback for the MATCH model.*

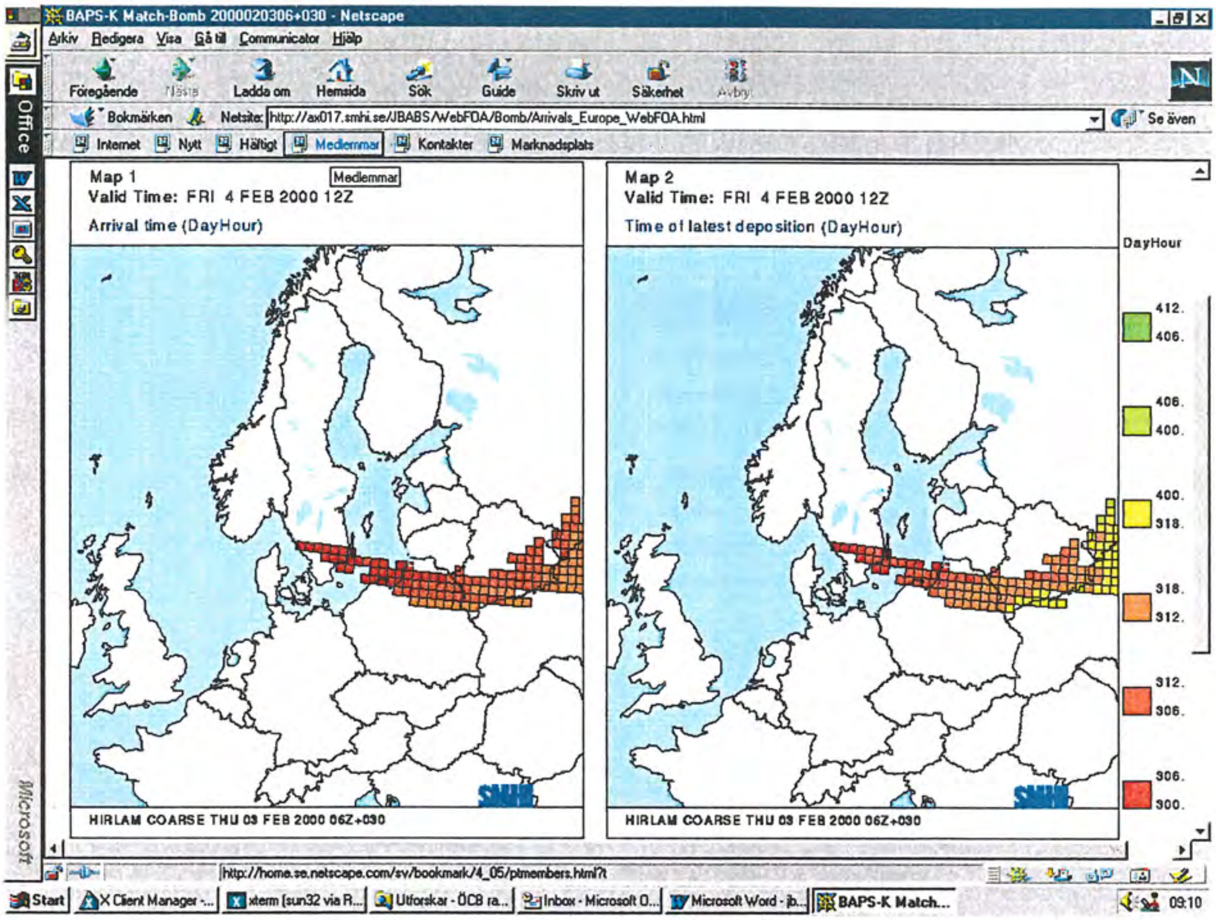

Figure A.8. An example of model results from MATCH and a nuclear weapon event. The figure shows arrival and latest time of radioactive deposition.

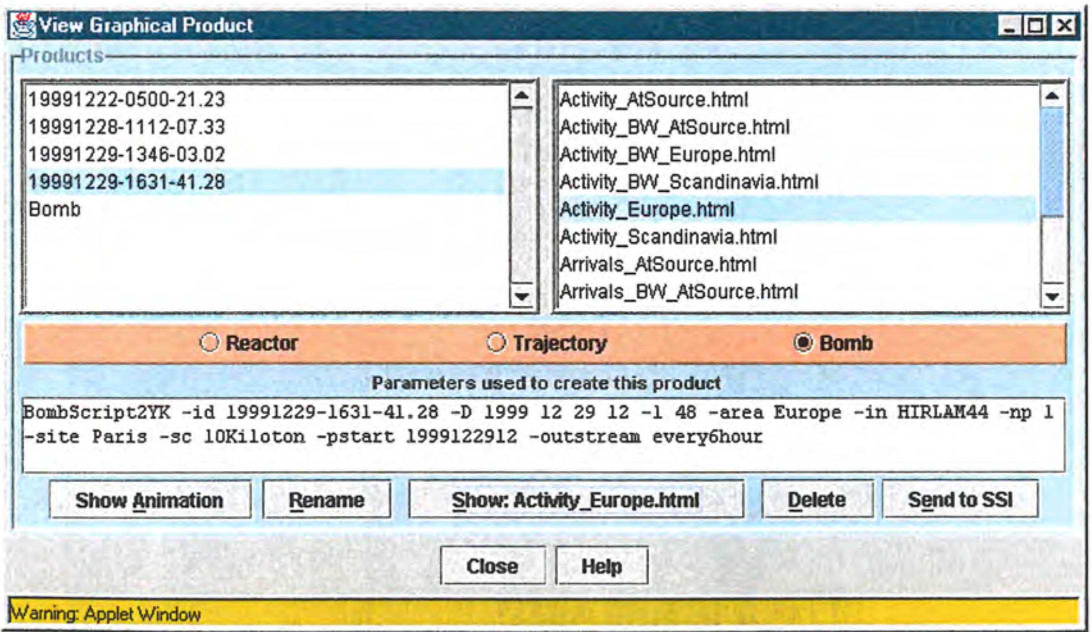

Figure A.9 Selection panel for viewing model results already produced.

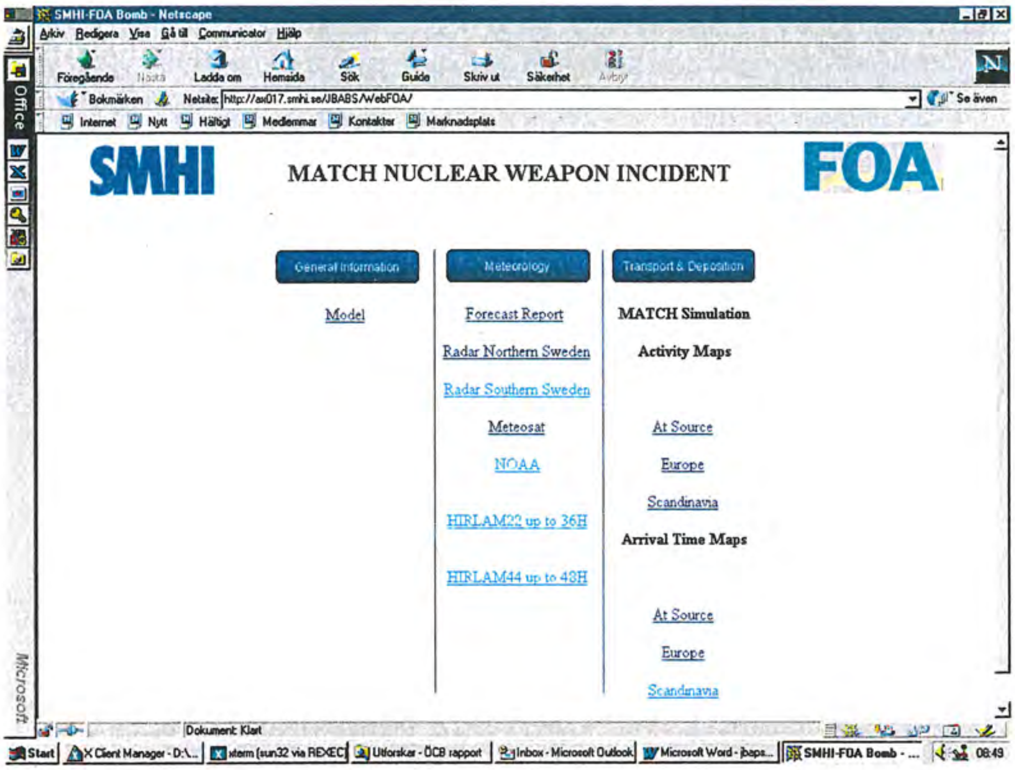

Figure A.10*. Real time presentation of weather information and transport model results on an Internet page with restricted access only for decision makers.*

SMHIs publiceringar

SMHI ger ut sex rapportserier. Tre av dessa, R-serierna är avsedda för internationell publik och skrivs därför oftast på engelska. I de övriga serierna används det svenska språket.

Seriernas namn	**Publiceras sedan**
RMK (Rapport Meteorologi och Klimatologi)	1974
RH (Rapport Hydrologi)	1990
RO (Rapport Oceanografi)	1986
METEOROLOGI	1985
HYDROLOGI	1985
OCEANOGRAFI	1985

I serien METEOROLOGI har tidigare utgivits:

1985

1 Hagmarker, A. (1985)
Satellitmeteorologi.

2 Fredriksson, U., Persson, Ch., Laurin, S. (1985)
Helsingborgsluft.

3 Persson, Ch., Wern, L. (1985)
Spridnings- och depositionsberäkningar för av fallsförbränningsanläggningar i Sofielund och Högdalen.

4 Kindell, S. (1985)
Spridningsberäkningar för SUPRAs anläggningar i Köping.

5 Andersson, C., Kvick, T. (1985)
Vindmätningar på tre platser på Gotland. Utvärdering nr 1.

6 Kindell, S. (1985)
Spridningsberäkningar för Ericsson, Ingelstafabriken.

7 Fredriksson, U. (1985)
Spridningsberäkningar för olika plymlyft vid avfallsvärmeverket Sävenäs.

8 Fredriksson, U., Persson, Ch. (1985)
NO_x- och NO_2-beräkningar vid Vasaterminalen i Stockholm.

9 Wern, L. (1985)
Spridningsberäkningar för ASEA transformers i Ludvika.

10 Axelsson, G., Eklind, R. (1985)
Ovädret på Östersjön 23 juli 1985.

11 Laurin, S., Bringfelt, B. (1985)
Spridningsmodell för kväveoxider i gatumiljö.

12 Persson, Ch., Wern, L. (1985)
Spridnings- och depositionsberäkningar för avfallsförbränningsanläggning i Sofielund.

13 Persson, Ch., Wern, L. (1985)
Spridnings- och depositionsberäkningar för avfallsförbränningsanläggning i Högdalen.

14 Vedin, H., Andersson, C. (1985)
Extrema köldperioder i Stockholm.

15 Krieg, R., Omstedt, G. (1985)
Spridningsberäkningar för Volvos planerade bilfabrik i Uddevalla.

16 Kindell, S. Wern, L. (1985)
Luftvårdsstudie avseende industrikombinatet i Nynäshamn (koncentrations- och luktberäkningar).

17 Laurin, S., Persson, Ch. (1985)
Beräknad formaldehydspridning och deposition från SWEDSPANs spånskivefabrik.

18 Persson, Ch., Wern, L. (1985)
Luftvårdsstudie avseende industrikombinatet i Nynäshamn – depositionsberäkningar av koldamm.

19 Fredriksson, U. (1985)
Luktberäkningar för Bofors Plast i Ljungby, II.

20 Wern, L., Omstedt, G. (1985)
Spridningsberäkningar för Volvos planerade bilfabrik i Uddevalla - energicentralen.

21 Krieg, R., Omstedt, G. (1985)
Spridningsberäkningar för Volvos planerade bilfabrik i Uddevalla - kompletterande beräkningar för fabrikerna.

22 Karlsson, K.-G. (1985)
Information från Meteosat - forskningsrön och operationell tillämpning.

23 Fredriksson, U. (1985)
Spridningsberäkningar för AB Åkerlund & Rausings fabrik i Lund.

24 Färnlöf, S. (1985)
Radarmeteorologi.

25 Ahlström, B., Salomonsson, G. (1985)
Resultat av 5-dygnsprognos till ledning för isbrytarverksamhet vintern 1984-85.

26 Wern, L. (1985)
Avesta stadsmodell.

27 Hultberg, H. (1985)
Statistisk prognos av yttemperatur.

1986

1 Krieg, R., Johansson, L., Andersson, C. (1986)
Vindmätningar i höga master, kvartalsrapport 3/1985.

2 Olsson, L.-E., Kindell, S. (1986)
Air pollution impact assessment for the SABAH timber, pulp and paper complex.

3 Ivarsson, K.-I. (1986)
Resultat av byggväderprognoser - säsongen 1984/85.

4 Persson, Ch., Robertson, L. (1986)
Spridnings- och depositionsberäkningar för en sopförbränningsanläggning i Skövde.

5 Laurin, S. (1986)
Bilavgaser vid intagsplan - Eskilstuna.

6 Robertson, L. (1986)
Koncentrations- och depositionsberäkningar för en sopförbränningsanläggning vid Ryaverken i Borås.

7 Laurin, S. (1986)
Luften i Avesta - föroreningsbidrag från trafiken.

8 Robertson, L., Ring, S. (1986)
Spridningsberäkningar för bromcyan.

9 Wern, L. (1986)
Extrema byvindar i Orrefors.

10 Robertson, L. (1986)
Koncentrations- och depositionsberäkningar för Halmstads avfallsförbränningsanläggning vid Kristinehed.

11 Törnevik, H., Ugnell (1986)
Belastningsprognoser.

12 Joelsson, R. (1986)
Något om användningen av numeriska prognoser på SMHI (i princip rapporten till ECMWF).

13 Krieg, R., Andersson, C. (1986)
Vindmätningar i höga master, kvartalsrapport 4/1985.

14 Dahlgren, L. (1986)
Solmätning vid SMHI.

15 Wern, L. (1986)
Spridningsberäkningar för ett kraftvärmeverk i Sundbyberg.

16 Kindell, S. (1986)
Spridningsberäkningar för Uddevallas fjärrvärmecentral i Hovhult.

17 Häggkvist, K., Persson, Ch., Robertson, L (1986)
Spridningsberäkningar rörande gasutsläpp från ett antal källor inom SSAB Luleåverken.

18 Krieg, R., Wern, L. (1986)
En klimatstudie för Arlanda stad.

19 Vedin, H. (1986)
Extrem arealnederbörd i Sverige.

20 Wern, L. (1986)
Spridningsberäkningar för lösningsmedel i Tibro.

21 Krieg, R., Andersson, C. (1986)
Vindmätningar i höga master - kvartalsrapport 1/1986.

22 Kvick, T. (1986)
Beräkning av vindenergitillgången på några platser i Halland och Bohuslän.

23 Krieg, R., Andersson, C. (1986)
Vindmätningar i höga master - kvartalsrapport 2/1986.

24 Persson, Ch. (SMHI), Rodhe, H. (MISU), De Geer, L.-E. (FOA) (1986)
Tjernobylolyckan - En meteorologisk analys av hur radioaktivitet spreds till Sverige.

25 Fredriksson, U. (1986)
Spridningsberäkningar för Spendrups bryggeri, Grängesberg.

26 Krieg, R. (1986)
Beräkningar av vindenergitillgången på några platser i Skåne.

27 Wern, L., Ring, S. (1986)
Spridningsberäkningar, SSAB.

28 Wern, L., Ring, S. (1986)
Spridningsberäkningar för ny ugn, SSAB II.

29 Wern, L. (1986)
Spridningsberäkningar för Volvo Hallsbergverken.

30 Fredriksson, U. (1986)
SO_2-halter från Hammarbyverket kring ny arena vid Johanneshov.

31 Persson, Ch., Robertson, L., Häggkvist, K. (1986)
Spridningsberäkningar, SSAB - Luleåverken.

32 Kindell, S., Ring, S. (1986)
Spridningsberäkningar för SAABs planerade bilfabrik i Malmö.

33 Wern, L. (1986)
Spridningsberäkningar för svavelsyrafabrik i Falun.

34 Wern, L., Ring, S. (1986)
Spridningsberäkningar för Västhamnsverket HKV1 i Helsingborg.

35 Persson, Ch., Wern, L. (1986)
Beräkningar av svaveldepositionen i Stockholmsområdet.

36 Joelsson, R. (1986)
USAs månadsprognoser.

37 Vakant nr.

38 Krieg, R., Andersson, C. (1986)
Utemiljön vid Kvarnberget, Lysekil.

39 Häggkvist, K. (1986)
Spridningsberäkningar av freon 22 från Ropstens värmepumpverk.

40 Fredriksson, U. (1986)
Vindklassificering av en plats på Hemsön.

41 Nilsson, S. (1986)
Utvärdering av sommarens (1986) använda konvektionsprognoshjälpmedel.

42 Krieg, R., Kvick, T. (1986)
Vindmätningar i höga master.

43 Krieg, R., Fredriksson, U. (1986)
Vindarna över Sverige.

44 Robertson, L. (1986)
Spridningsberäkningar rörande gasutsläpp vid ScanDust i Landskrona - bestämning av cyanvätehalter.

45 Kvick, T., Krieg, R., Robertson, L. (1986)
Vindförhållandena i Sveriges kust- och havsband, rapport nr 2.

46 Fredriksson, U. (1986)
Spridningsberäkningar för en planerad panncentral vid Lindsdal utanför Kalmar.

47 Fredriksson, U. (1986)
Spridningsberäkningar för Volvo BMs fabrik i Landskrona.

48 Fredriksson, U. (1986)
Spridningsberäkningar för ELMO-CALFs fabrik i Svenljunga.

49 Häggkvist, K. (1986)
Spridningsberäkningar rörande gasutsläpp från syrgas- och bensenupplag inom SSAB Luleåverken.

50 Wern, L., Fredriksson, U., Ring, S. (1986)
Spridningsberäkningar för lösningsmedel i Tidaholm.

51 Wern, L. (1986)
Spridningsberäkningar för Volvo BM ABs anläggning i Braås.

52 Ericson, K. (1986)
Meteorological measurements performed May 15, 1984, to June, 1984, by the SMHI.

53 Wern, L., Fredriksson, U. (1986)
Spridningsberäkning för Kockums Plåtteknik, Ronneby.

54 Eriksson, B. (1986)
Frekvensanalys av timvisa temperaturobservationer.

55 Wern, L., Kindell, S. (1986)
Luktberäkningar för AB ELMO i Flen.

56 Robertson, L. (1986)
Spridningsberäkningar rörande utsläpp av NO_x inom Fagersta kommun.

57 Kindell, S. (1987)
Luften i Nässjö.

58 Persson, Ch., Robertson, L. (1987)
Spridningsberäkningar rörande gasutsläpp vid ScanDust i Landskrona - bestämning av cyanväte.

59 Bringfelt, B. (1987)
Receptorbaserad partikelmodell för gatumiljömodell för en gata i Nyköping.

60 Robertson, L. (1987)
Spridningsberäkningar för Varbergs kommun. Bestämning av halter av SO_2, CO, NO_x samt några kolväten.

61 Vedin, H., Andersson, C. (1987)
E 66 - Linderödsåsen - klimatförhållanden.

62 Wern, L., Fredriksson, U. (1987)
Spridningsberäkningar för Kockums Plåtteknik, Ronneby. 2.

63 Taesler, R., Andersson, C., Wallentin, C., Krieg, R. (1987)
Klimatkorrigering för energiförbrukningen i ett eluppvärmt villaområde.

64 Fredriksson, U. (1987)
Spridningsberäkningar för AB Åetå-Trycks planerade anläggning vid Kungens Kurva.

65 Melgarejo, J. (1987)
Mesoskalig modellering vid SMHI.

66 Häggkvist, K. (1987)
Vindlaster på kordahus vid Alviks Strand - numeriska beräkningar.

67 Persson, Ch. (1987)
Beräkning av lukt och föroreningshalter i luft runt Neste Polyester i Nol.

68 Fredriksson, U., Krieg, R. (1987)
En överskalig klimatstudie för Tornby, Linköping.

69 Häggkvist, K. (1987)
En numerisk modell för beräkning av vertikal momentumtransport i områden med stora råhetselement. Tillämpning på ett energiskogsområde.

70 Lindström, Kjell (1987)
Weather and flying briefing aspects.

71 Häggkvist, K. (1987)
En numerisk modell för beräkning av vertikal momentumtransport i områden med stora råhetselement. En koefficientbestämning.

72 Liljas, E. (1988)
Förbättrad väderinformation i jordbruket - behov och möjligheter (PROFARM).

73 Andersson, Tage (1988)
Isbildning på flygplan.

74 Andersson, Tage (1988)
Aeronautic wind shear and turbulence. A review for forecasts.

75 Kållberg, P. (1988)
Parameterisering av diabatiska processer i numeriska prognosmodeller.

76 Vedin, H., Eriksson, B. (1988)
Extrem arealnederbörd i Sverige 1881 - 1988.

77 Eriksson, B., Carlsson, B., Dahlström, B. (1989)
Preliminär handledning för korrektion av nederbördsmängder.

78 Liljas, E. (1989)
Torv-väder. Behovsanalys med avseende på väderprognoser och produktion av bränsletorv.

79 Hagmarker, A. (1991)
Satellitmeteorologi.

80 Lövblad, G., Persson, Ch. (1991)
Background report on air pollution situation in the Baltic states - a prefeasibility study.
IVL Publikation B 1038.

81 Alexandersson, H., Karlström, C., Larsson-McCann, S. (1991)
Temperaturen och nederbörden i Sverige 1961-90. Referensnormaler.

82 Vedin, H., Alexandersson, H., Persson, M. (1991)
Utnyttjande av persistens i temperatur och nederbörd för vårflödesprognoser.

83 Moberg, A. (1992)
Lufttemperaturen i Stockholm 1756 - 1990. Historik, inhomogeniteter och urbaniseringseffekt.
Naturgeografiska Institutionen, Stockholms Universitet.

84 Josefsson, W. (1993)
Normalvärden för perioden 1961-90 av globalstrålning och solskenstid i Sverige.

85 Laurin, S., Alexandersson, H. (1994)
Några huvuddrag i det svenska temperaturklimatet 1961 - 1990.

86 Fredriksson, U. och Ståhl, S. (1994)
En jämförelse mellan automatiska och manuella fältmätningar av temperatur och nederbörd.

87 Alexandersson, H., Eggertsson Karlström, C. och Laurin S. (1997).
Några huvuddrag i det svenska nederbördsklimatet 1961-1990.

88 Mattsson, J., Rummukainen, M. (1998)
Växthuseffekten och klimatet i Norden - en översikt.

89 Kindbom, K., Sjöberg, K., Munthe, J., Peterson, K. (IVL)
Persson, C. Roos, E., Bergström, R. (SMHI). (1998)
Nationell miljöövervakning av luft- och nederbördskemi 1996.

90 Foltescu, V.L., Häggmark, L (1998)
Jämförelse mellan observationer och fält med griddad klimatologisk information.

91 Hultgren, P., Dybbroe, Karlsson, K.-G. (1999)
SCANDIA – its accuracy in classifying LOW CLOUDS

92 Hyvarinen, O., Karlsson, K.-G., Dybbroe, A. (1999)
Investigations of NOAA AVHRR/3 1.6 μm imagery for snow, cloud and sunglint discrimination
(Nowcasting SAF)

93 Bennartz, R., Thoss, A., Dybbroe, A. and Michelson, D. B. (1999)
Precipitation Analysis from AMSU
(Nowcasting SAF)

94 Appelqvist, Peter och Anders Karlsson (1999)
Nationell emissionsdatabas för utsläpp till luft - Förstudie.

101 Josefsson, W. (1989)
Computed global radiation using interpolated, gridded cloudiness from the MESA-BETA analysis compared to measured global radiation.

SMHI

Swedish Meteorological and Hydrological Institute
SE 601 76 Norrköping, Sweden.
Tel +46 11-495 80 00. Fax +46 11-495 80 01

ISSN 0283-7730